



universität
wien

MAGISTERARBEIT

Titel der Magisterarbeit

Search for Additional Bodies with the Transit
Timing Method

angestrebter akademischer Grad

Magistra der Naturwissenschaften (Mag. rer. nat.)

Verfasserin: Monika Lendl Bakk. rer. nat.
Matrikel-Nummer: 0404319
Studienrichtung: Astronomie
Betreuer: Priv. Doz. Mag. Dr. Gerald Handler

Wien, im November 2009

Gewidmet meinen Eltern

Contents

Abstract	7
Deutsche Zusammenfassung	9
1 Introduction	11
1.1 The Study of Extrasolar Planets	12
1.1.1 Pulsar Planets	12
1.1.2 The First Planets around Main-Sequence Stars	12
1.1.3 The Next Step: Transits	14
1.1.4 Looking for Distant Planets with Microlensing	14
1.1.5 Finding Elements in Exoplanet Atmospheres	15
1.1.6 The First Images of Extrasolar Planets	15
1.1.7 Towards Earth-like Planets	16
1.2 Transiting Extrasolar Planets	18
1.2.1 Transit Searches	19
1.2.2 The Transiting Exoplanet Sample	21
1.2.3 Other Properties Accessible for Transiting Exoplanets	23
1.3 Layout of the Thesis	24
2 The Transit Timing Variations Technique	25
2.1 The Transit Timing Method	25
2.2 Results of Previous Searches	28
2.3 Future Perspectives	28
3 Observations and Data Reduction	31
3.1 Observations	31
3.1.1 Target and Site Selection	31
3.1.2 Observation Strategy	32
3.1.3 Observing Process	32
3.2 Data Reduction	33
3.2.1 Basic Image Reduction	34
3.2.2 Instrument-Specific Image Correction	35
3.2.3 Aperture Photometry with IRAF and Manual Creation of a Reference Source	35

3.2.4	Aperture Photometry with <i>mupipe</i>	37
3.2.5	Comparison	37
4	Determination of System Parameters	43
4.1	The Model	43
4.2	The Fitting Routine	45
4.2.1	Overview of the Fitting Process	45
4.2.2	The Fitting Programs	46
4.3	Error Calculation	48
4.3.1	The Bootstrap Monte Carlo Method	48
4.3.2	The χ^2 Surface	49
5	Results	51
5.1	Planetary Parameters	51
5.1.1	Wavelength Dependency of the Results	51
5.1.2	Dependence on the Limb Darkening Coefficients	53
5.1.3	Comparison to Previously Published Values	54
5.2	New Ephemeris and Transit Timing Variations	55
5.2.1	An Improved Ephemeris	55
5.2.2	Transit Timing Variations	56
6	Conclusion	61
	Bibliography	72
	Acknowledgments	73

Abstract

Among the currently known extrasolar planets, 62 systems are aligned in a way so that the planet passes in front of the star once per orbit. As this happens, the planet occults part of the stellar disk, and a dip in the star's brightness can be measured. The study of these transiting systems allows us to determine fundamental properties of the planet, namely the true mass, the radius and the orbital inclination. As the transit depth decreases with the square of the planetary radius and the transit probability decreases with the orbital separation, it is very difficult to detect transiting Earth-like planets. However, transits allow us to measure the period of the transiting planet with good accuracy and enable us to detect small period variations caused by the gravitational impact of additional bodies in the system. This way, even Earth-sized objects can, theoretically, be found.

In this work, I probe the OGLE2-TR-L9 planetary system which contains a close-in gas giant (a so-called "Hot Jupiter"), for such variations. For this purpose, five transits of OGLE2-TR-L9 were recorded at the MPI/ESO 2.2m telescope at La Silla observatory using the GROND multi-channel imager which observes simultaneously in four optical and three infrared filters. These observations allow us to redetermine the parameters of OGLE2-TR-L9 b which itself is a largely unstudied planet.

The first step in determining the planetary parameters and mid-transit times is the data reduction which encompasses the image correction and the production of a light curve. For this purpose, the software packages *IRAF* and *mupipe* were used together with some purposely made IDL routines. Then, the planetary parameters are determined by fitting a theoretical model of a planetary transit in the observed light curves. Here, the best fitting parameters are found using a downhill simplex method.

The results of these new observations of OGLE2-TR-L9 do not agree with the previously published values. In section 5, the discrepancies are discussed and reasons are given for the accuracy of the new parameters. Further, the wavelength dependencies of the results are investigated. To search for transit timing variations, the measured mid-transit times are divided into two subsets and investigated separately. No conclusive detection of transit timing variations has been made but at the same time, the presence of such variations can not be excluded and further observations are encouraged to answer this question.

Zusammenfassung

Unter den derzeit bekannten extrasolaren Planeten gibt es eine Anzahl von Systemen, deren Umlaufebenen so ausgerichtet sind, dass sie die Sichtlinie auf den Stern durchkreuzen. Passiert dies, so wird für kurze Zeit durch den Planeten ein Teil der Sternscheibe verdeckt und für den Beobachter ist eine kurzzeitige Verdunkelung des Sterns messbar. Das Studium dieser planetaren Transits bietet uns die Möglichkeit, fundamentale Parameter des Planeten, nämlich Masse, Radius und Bahninklination, festzulegen. Da die Tiefe des beobachteten Transits mit dem Quadrat des Planetenradius abnimmt, und die Transitwahrscheinlichkeit mit dem Bahnradius abnimmt, ist die Entdeckung von erdähnlichen Planeten mit Transits sehr schwierig. Allerdings eröffnen uns Transits die Möglichkeit, die Periode des Planeten mit großer Genauigkeit zu messen und dadurch kleine Variationen in dieser festzustellen, Variationen die durch den gravitativen Einfluss weiterer Körper im Planetensystem (insbesondere weiterer eventuell erdähnlicher Planeten) entstehen können.

In dieser Arbeit untersuche ich das Planetensystem OGLE2-TR-L9, das einen sogenannten „Hot Jupiter“, einen Gasriesen auf einer sehr engen Umlaufbahn besitzt, nach derartigen Variationen. Zu diesem Zweck wurden mit dem MPI/ESO 2.2m Teleskop auf La Silla fünf Transits von OGLE2-TR-L9 aufgenommen. Das verwendete Instrument, GROND, erlaubt die gleichzeitige Beobachtung in 4 optischen und 3 infrarot- Filtern. Diese Beobachtungen ermöglichen es auch die Parameter des Planeten OGLE2-TR-L9 b, welcher noch nahezu unerforscht ist, neu zu bestimmen.

Der erste Schritt in der Bestimmung der Planetenparameter und Mittransitzeiten besteht in der Auswertung der Daten, die von der Bildkorrektur bis zur Erstellung der Lichtkurven, in welchen die Helligkeit des Sterns gegen die Zeit aufgetragen ist, reicht. Für diesen Schritt wurden sowohl die Softwarepakete *IRAF* und *mupipe* als auch eigens geschriebene Routinen verwendet. Darauf folgt die Bestimmung der Planetenparameter, indem die passendsten Parameter mit einem theoretischen Modell für Planetentransits bestimmt werden. Zu diesem Zweck wurde die Simplex Methode verwendet.

Die Resultate der neuen Beobachtungen von OGLE2-TR-L9 decken sich nicht mit den bisher publizierten Werten. In Abschnitt 5 werden die Unterschiede diskutiert und Gründe für die Glaubwürdigkeit der hier bestimmten Werte angeführt. Weiters werden die Resultate auf Abhängigkeit bezüglich der Wellenlänge unter-

sucht. Zur Suche nach Periodenvariationen werden die vorhandenen Datenpunkte in zwei Untergruppen eingeteilt und separat nach Variationen untersucht. Es können keine eindeutigen Hinweise für Periodenvariationen identifiziert werden, jedoch sind derartige Variationen nicht auszuschließen und weitere Messungen sind nötig um eine fundierte Aussage treffen zu können.

Chapter 1

Introduction

Over the course of centuries of astronomical research, few subjects have captured the public as well as scientists as much as the search for and study of extrasolar planets. For many generations the thought of planets orbiting stars other than the sun, possibly inhabited by creatures not too different from the human race itself, has been inspiring to arts of all disciplines. Still, up to the 1990ies, these ideas have been out of reach of actual scientific investigation, a subject that was left to the arts to explore.

While, for many of us, the search for planets is motivated by the desire to discover places which are similar to our home planet and might be havens for alien life, the endeavor in searching for distant worlds is not only a quest for discovery and understanding, it is also a discipline in astronomy which keeps pushing the limits of science and technology. For the discovery and study of planets around other stars, new techniques need to be devised and new instrumentation has to be developed. While, 20 years ago, the first discovery of extrasolar planets was yet to come, we now know more than 400 of these objects and have progressed to studying their composition and to discovering small objects. But not only have we learned a lot from these discoveries, in fact the discoveries have turned out to be very different from both, the visions of artists and scientific expectations. While most researchers expected to find planetary systems much resembling our own solar system, the discoveries show quite a different picture, revolutionizing our understanding of planetary systems, pushing us to explain the existence of objects more massive than Jupiter but 20 times closer to their star than Mercury to our Sun, objects on orbits that are highly eccentric and planets located in binary star systems. As a consequence the subject of extrasolar planets has become not only a question of discoveries and thus technology but also very much a subject of theoretical research.

This work should be seen as a small part in the strife to broaden or understanding of planetary systems and the occurrence of planets around stars other than the Sun, pushing to discover small, possibly even Earth-like planets. For this purpose, I implement a recently proposed technique to detect small planets in systems

containing one known transiting planet.

1.1 The Study of Extrasolar Planets

1.1.1 Pulsar Planets

Although one usually refers to the discovery of a planet orbiting the star 51 Peg (Mayor and Queloz, 1995) as the first discovery of an exoplanet, the first planet-like object known to orbit a star was found in 1992 by Wolszczan and Frail. In their paper, the discovery of two Earth-sized objects orbiting a pulsar is reported. The detection was based on irregularities in the observed pulsar frequency which are caused by the variable light travel time due to the motion of the pulsar around the barycenter of the “planetary” system. The reason why these planets are usually discussed separately from planets around main-sequence stars is twofold, on one hand, the detection technique is different from the techniques used to discover planets around main-sequence stars, but more importantly, the pulsar planets are a whole different class of objects which are believed to have formed after the supernova explosion of the star (see Phinney and Hansen, 1993; Currie and Hansen, 2007; Hansen et al., 2009).

1.1.2 The First Planets around Main-Sequence Stars

The first planet orbiting a main-sequence star was discovered by searching the host star, 51 Peg, for variations in its radial velocity (Mayor and Queloz, 1995). As with pulsar timing, these variations are attributed to the motion of the star around the barycenter of the planetary system, and accordingly this technique is dubbed the *radial velocity method*. The newly discovered planet itself turned out to be quite different from what scientists expected to find in exoplanetary systems: 51 Peg b is a $0.47M_J$ planet orbiting a G-type star with a period of merely 4.32 days. In the following years, a gradually increasing number of discoveries were made, all using the radial velocity method (Butler et al., 1997; Cochran et al., 1997; Noyes et al., 1997 to name a few) finding a considerable number of close-in planets as well as planets at larger separations. In a few cases, even multi planet systems were identified (e.g. Lissauer, 1999). These close-in giant planets are often dubbed “Pegasides” after 51 Peg b or “Hot Jupiters” according to their physical properties. In the light of this first sample of planets, it is important to point out that the radial-velocity technique itself favors the detection of massive close-in planets since they produce pronounced radial velocity variations on easily accessible timescales. Since with the radial velocity method only the radial velocity component of the star’s total velocity is measured, the mass can only be determined with this limitation, and thus the masses determined with radial velocity are given as $m \sin(i)$, where i is the inclination of the orbit. Another unexpected feature found in the newly discovered planets are their eccentricities which are in some cases substantially larger than expected, possibly hinting at a turbulent past. To summarize the first five years of

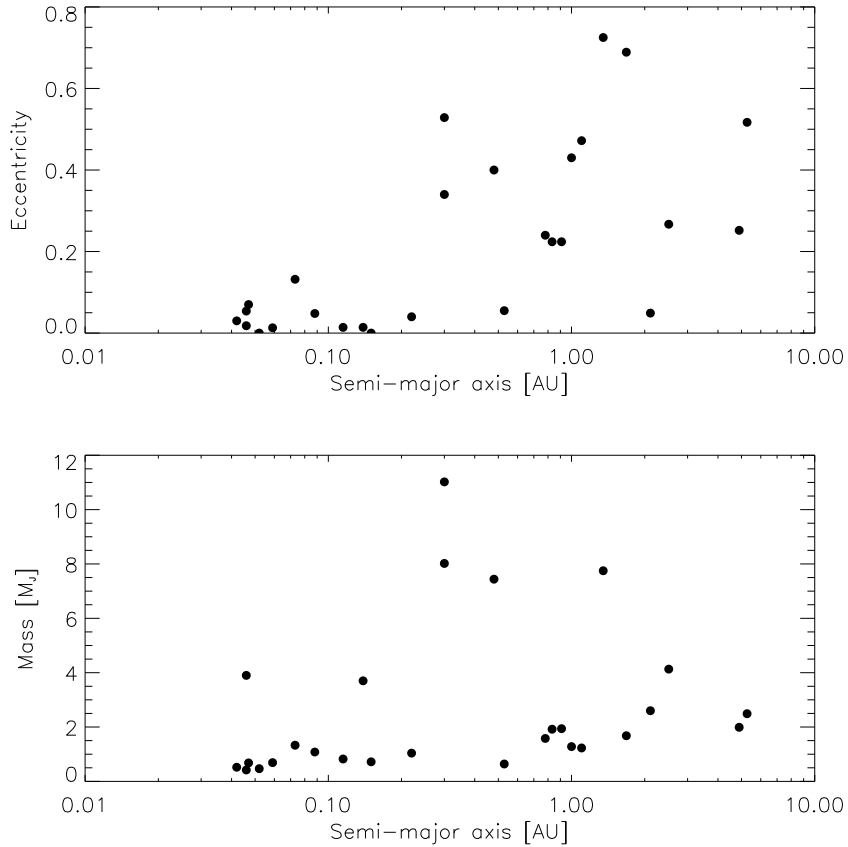


Figure 1.1: The parameters of all exoplanets around main-sequence stars discovered before 2000. In the upper panel, the eccentricity is plotted versus the semi-major axis. It can be seen that, with increasing semi-major axis, high eccentricity planets are present. In the lower panel, the planetary mass versus the planetary semi-major axis is depicted. Here the Pegasides with separations of less than 0.1 AU are visible. Also note that at this point in time only planets with masses comparable to that of Jupiter or larger could be detected.

detections, Figure 1.1 shows the semi-major axis versus eccentricity ($a - e$) and the semi-major axis versus mass ($a - M$) diagram of all planets detected until 2000. Note that the abscissa is depicted in a logarithmic scale for reasons of clarity.

1.1.3 The Next Step: Transits

Once the existence and detectability of planets orbiting other stars had been established, a growing interest arose to find systems which are viewed edge-on so that the planet passes in front of the stellar disk, thereby producing a signature similar (although much smaller) to that of an eclipsing binary. The transit depth caused by a Hot Jupiter is in the range of one percent, thus easily detectable, making it only a matter of time until a system with an inclination close enough to 90° was found. This was the case for the planet HD 209458b which was discovered to transit in 1999 (Charbonneau et al. (2000), Henry et al. (2000)).

The measurement of planetary transits allows us to determine several parameters which are not accessible by other means, shedding more light on the nature of the transiting planet. Just from the transit light curve itself, the planetary radius and the inclination of the orbit can be found by investigating shape and depth of the transit light curve. Together with radial velocity measurements, knowledge of the inclination allows us to determine the true mass of the planet. The true mass can then be used in conjunction with the radius to find the mean density of the planet allowing to constrain the planet's composition and structure. The major disadvantage of the transit method is that it suffers from some strong observational biases: for geometrical reasons, the transit probability decreases with the orbital separation and the transit becomes shallower for small planets, reaching down to a dimming of only 0.01% for Earth-like planets. Another factor which favors the discovery of short-period transiting planets is the large amount of observing time needed to identify a transiting planet with a period of more than a few days as the transit has to be observed repeatedly. Strategies to overcome these restrictions will be described in section 1.2.

While the transit of HD 209458, a planet which had been discovered with the radial velocity method, proved that it is possible to observe transits, it was yet to evaluate whether the search for transits could be used as an effective method to discover exoplanets. It took until 2002 for the first planet to be identified primarily from photometric data (Udalski et al., 2002; Konacki et al., 2003). Until the first dedicated surveys started producing results (e.g. Alonso et al., 2004; Bakos et al., 2007) there was only a small number of transiting planets, mainly Hot Jupiters, known.

1.1.4 Looking for Distant Planets with Microlensing

The detection methods described above are both indirect, involving only the information about the planet which is contained in the light of the star and do not need any detection of the planet itself. The microlensing method takes these indirect ob-

servations one step further: now not even the planet host star needs to be seen. The idea is that, especially when observing towards the galactic center, it can happen that a faint star passes in front of a luminous background star. The passing star acts as a gravitational lens, increasing the amount of light reaching the observer for a short time. Should the passing star have a planetary companion, it can show up on the obtained light curve as additional spikes. This method was first applied successfully by Bond et al. (2004), detecting an $1.5M_J$ planet at an orbital radius of approximately 3 AU. Since then, a handful of planets with masses down to about $3.7M_{\oplus}$ (Bennett et al., 2008) have been discovered in this way. The obvious disadvantage of the microlensing technique is that each detection is only made once and cannot be repeated.

1.1.5 Finding Elements in Exoplanet Atmospheres

The discovery of transiting extrasolar planets opened the door to, for the first time, investigating their composition. The first detection of the presence of elements in the planetary atmosphere of a transiting planet, namely HD 209458b, was performed by Charbonneau et al. (2002) when observations during transit revealed absorption of sodium in the planet's atmosphere. This discovery has been followed by an increasing number of detections in the last few years, which have implemented essentially two different techniques. On one hand, observations during transit reveal absorption features produced by the planetary atmosphere, which allowed to detect among others e.g. the presence of water in HD 209458b (Beaulieu et al., 2009) and HD 189733 b (Tinetti et al., 2007). On the other hand, it is possible to gain insights on the planet's atmospheric composition by observing shortly before/after and during the secondary eclipse. Comparing the obtained measurements (which usually are spectra binned to a low spectral resolution), the contribution from the planet can be identified. This technique has proven successful on a number of accounts, such as the detection of CO_2 , CO and H_2O on HD 189733 (Swain et al., 2008) and the detection of silicate clouds on HD 209458 (Richardson et al., 2007).

1.1.6 The First Images of Extrasolar Planets

There has always been a large motivation to be able to actually detect the light coming from an extrasolar planet, and use it to take a picture. Apart from its inspirational value, the direct imaging technique allows us to discover planets at large orbital separations, a regime which is not accessible with the indirect methods. Direct imaging usually is done in the infrared and for young stars since the contrast between star and planet is smaller in the IR and planets are believed to be brightest at young ages. Up to now only a handful of objects have been identified. Until October 2008 the detected systems were either brown dwarfs orbiting stars (Chauvin et al., 2005; Biller et al., 2006; Schmidt et al., 2008) or brown dwarfs orbited by planets (Chauvin et al., 2004; Neuhäuser et al., 2005). But in late 2008,

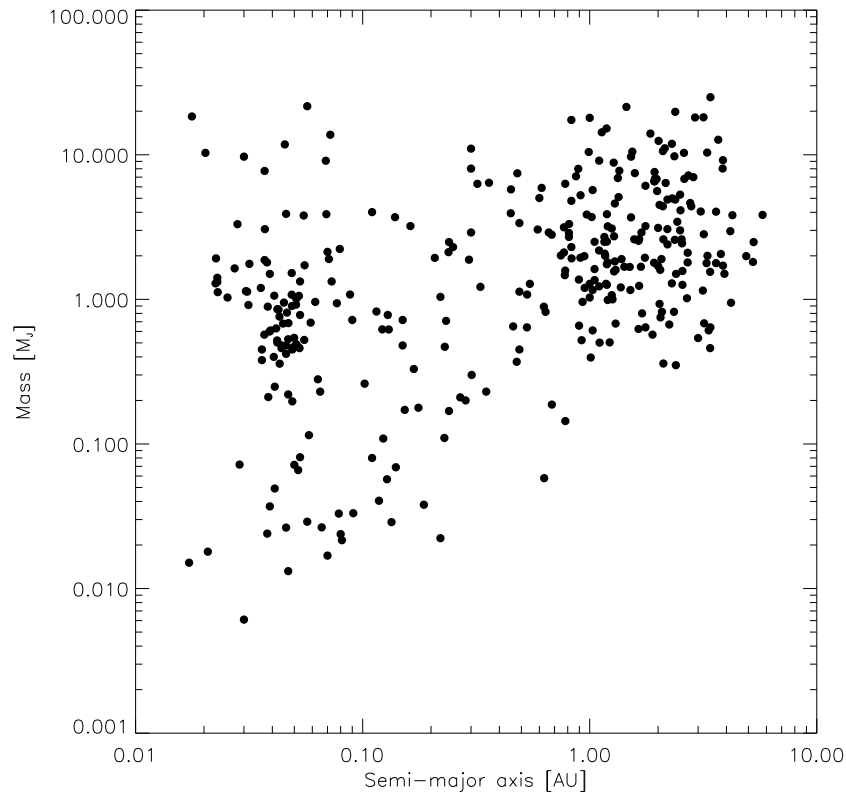


Figure 1.2: The parameters (planet mass versus orbital separation) of all exoplanets around main-sequence stars discovered until mid-2009 are depicted. Now, the newly discovered low-mass planets can be seen in the lower part of the diagram. Note that so far small planets have only been discovered at small orbital separations, an effect of the observational biases of the radial velocity and transit methods.

companions were detected around the stars β Pic (Lagrange et al., 2009), Fomalhaut (Kalas et al., 2008) and HR 8799 (Marois et al., 2008). The Fomalhaut- and HR 8799 systems deserve special attention as Fomalhaut b has been observed in the optical with the Hubble Space Telescope and HR 8799 hosts not one but three confirmed planets.

1.1.7 Towards Earth-like Planets

Discovering an extrasolar planet with characteristics almost identical to the Earth has always been some sort of a holy grail in exoplanet sciences. Sure enough, an Earth-twin is not easy to find, since it is small and orbits its parent star at quite a large separation, a parameter space where the common techniques are not very

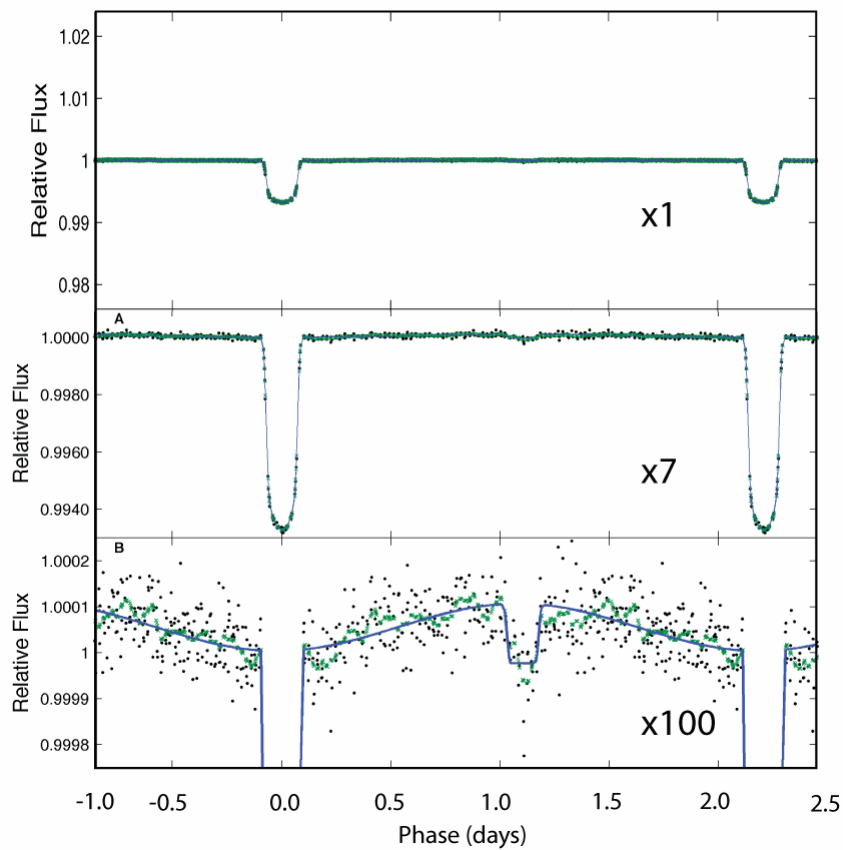


Figure 1.3: The transit and secondary eclipse of HAT-P-7 recorded by Borucki et al. (2009) with the Kepler satellite. Note the excellent quality of the photometry allowing to see the eclipse in the optical and the intensity variation caused by the reflected starlight.

sensitive. Nevertheless, some considerable advances have been made in the radial velocity and transit techniques putting us in a position where the discovery of an alien Earth is clearly within reach. The new possibilities in discovering low mass planets are reflected in the current a - M diagram (figure 1.2). Over the last 10 years, the number of known extrasolar planets has risen beyond 400. The reason for this drastic increase can be found in the increasing number and accuracy of radial-velocity and transit planet searches.

In recent years, several systems hosting so called super-Earths (i. e. planets of a few Earth-masses) have been discovered, mainly by the HARPS Planet search program (Pepe et al., 2002) which uses the radial-velocity technique. At the current time, the least massive exoplanet known to orbit a main sequence star is GJ 581 e with a minimum mass of $m \sin i = 1.9M_{\oplus}$ (Mayor et al., 2009). It is located in a 4-planet system, with the other companions being a one Neptune-sized planet (planet b) and two super-Earths (planets c and d), around an M dwarf (Bonfils et al., 2005; Udry et al., 2007). The planets c and d of this system are located in the habitable zone making it, theoretically, possible for liquid water to exist on their surfaces.

While the radial velocity technique is able to detect Earth-sized planets it is still up to the transit-technique to determine the true mass and mean density of the planet and thus find out whether it is of rocky nature. While the necessary accuracy to detect super-Earth transits has not been achieved with ground based observations, the recent launches of satellites capable of high accuracy photometry, namely CoRoT (Bordé et al., 2003) and Kepler (Koch et al., 1998), have opened up new possibilities in transit discoveries. Recently, a planet with a mass of $4.8 \pm 0.8M_{\oplus}$ (Queloz et al., 2009) and a radius of $1.65 \pm 0.09R_{\oplus}$ (Leger et al., 2009) was found to transit a K0V star by the CoRoT satellite. Radial-velocity measurements of this system showed the system hosts a second non-transiting companion with a mass of $8.4 \pm 0.9M_{\oplus}$ (Queloz et al., 2009). While the accuracy of CoRoT is not good enough to detect planets having one Earth-radius, the newest photometry satellite, Kepler has recently proven that it is capable of reaching the necessary accuracy by observing the secondary eclipse of the $\sim 1.5M_J$ planet HAT-P-7 at optical wavelengths (Borucki et al., 2009). The light curve recorded by Kepler is shown in Figure 1.3. Judging from these recent developments, I believe that it does not require great optimism to assume that the discovery of the first exo-Earth is drawing very near.

1.2 Transiting Extrasolar Planets

In the study of extrasolar planets, the observation of planetary transits has a prominent position. As described in section 1.1.3, transiting exoplanets allow us to gain many more insights than their radial-velocity-only counterparts. I will not elaborate on the details of the transit technique here since the procedure to determine the planetary parameters from the light curve is described in detail in section 4.1. It however still remains to discuss the observational strategies to implement the tran-

sit method for the discovery and characterization of a large number of exoplanets (section 1.2.1) and to give details about the transiting exoplanet sample and the insights gained from it (section 1.2.2).

1.2.1 Transit Searches

While the first transits were found from the observation of planets previously detected by radial velocity, the transit technique has by now become a main player in the discovery of exoplanets. The search for exoplanets via planetary transits is carried out via photometric surveys which observe a large number of stars. Since the transit probability of a planet decreases with R_*/a_{sm} , especially for the discovery of further-out planets, a large star sample has to be observed in order to be able to expect a reasonable number of detections. Further out planets however, pose one more challenge, next to their low transit probability, as they have long periods and thus the star needs to be observed for a longer timespan to confirm the transit. In the following, I will discuss the various transit searches that have led to the successful identification of transiting exoplanets.

Ground-based Transit Searches

The ground-based transit searches can be divided into two subgroups. While some searches are working with simple cameras equipped with lenses of about 10 - 20 cm having large fields of view but only reaching the necessary precision for bright stars, other searches are working with larger telescopes, probing smaller fields but reaching down to about the 17th magnitude. Independent of their nature, the ground based transit searches usually use a small number of telescopes located on different continents in order to achieve a maximum time coverage.

HAT Net The **Hungarian Automatic Telescope Network** uses three sites. There are cameras installed at Manua Kea (Hawaii) and FLWO (Arizona) (“HAT”) together with a camera (“WHAT”) at WISE Observatory (Israel). HAT Net is a shallow wide angle (approx. $8^\circ \times 8^\circ$) survey with telescopes of an aperture of 11 cm (HAT) and 20 cm (WHAT) At the time of writing, three additional sites on the southern hemisphere (Chile, Namibia, Australia) were under construction (Bakos et al., 2009a). HAT Net is one of the most successful transit surveys with 13 confirmed detections.

TrES TrES, short for **Transatlantic Exoplanet Survey**, uses telescopes at three sites: Tenerife (The Canary Islands), Lowell Observatory (Arizona) and Mount Palomar (California). The telescopes have an aperture of 10 cm and the field of view is 6° (Alonso et al., 2004) making it a shallow survey which has successfully discovered 4 planets.

SuperWASP Unlike HAT or TrES, SuperWASP (short for **Wide Angle Search for Planets**) has only one site in each hemisphere, La Palma (Canary Islands) and

SAAO (South Africa). Each site is equipped with eight off-the-shelf cameras of an aperture of 11.1 cm covering a total field of view of 482 square degrees (Pollacco et al., 2006). The SuperWASP project has been highly successful, discovering a total of 18 transiting exoplanets.

XO XO is the smallest of the successful wide-angle searches, having only two cameras installed at Haleakala Summit on Maui (Hawaii). The cameras each have a lens diameter of 20 cm and a field of view of $7.2^\circ \times 7.2^\circ$ (McCullough et al., 2005). So far, 5 planets have been identified by XO.

OGLE OGLE, short for **O**ptical **G**ravitational **L**ensing **E**xperiment was initially devised with the aim to detect microlensing events to study the distribution of dark matter but has expanded to investigate variable stars including planetary transits. For this purpose, the 1.3m Warsaw telescope at Las Campanas observatory (Chile) is used to observe fields of $35' \times 35'$ making it a deep but narrow-angle survey. The third phase of the OGLE-project, OGLE-III was especially adapted to the discovery of transiting exoplanets and succeeded in discovering the first exoplanet discovered with the transit method (Udalski et al., 1997, 2003). Recently, a transiting planet, OGLE2-TR-L9 has been identified in data from the second phase of the OGLE-project (Snellen et al., 2009). Several newly observed transits of this object will be presented in this work.

Space-based Transit Searches

Naturally, the ground-based observations suffer from limitations due to restricted visibility times and atmospheric conditions, problems which can be bypassed by going to space. With a new generation of purpose-dedicated photometry satellites, we are now able to observe fields continuously for several months with high photometric precision, pushing the limits of the transit method towards smaller planets and larger orbital separations.

SWEEPS The first published detection of extrasolar planets from space was done with the **S**agittarius **W**indow **E**clipsing **E**xtrasolar **P**lanet **S**earch which conducted photometric observations of a field in the galactic bulge using the Hubble Space Telescope. Two stars with magnitudes of $mag_V = 18.8$ and $mag_V = 19.8$ were proposed as planet host stars (Sahu et al., 2006). However, at these magnitudes, the possibilities for spectroscopic confirmation are limited.

CoRoT The **C**onvection, **R**otation and exoplanet **T**ransit Satellite CoRoT was launched into a polar orbit 2006. It has an aperture of 27 cm and four CCD cameras, two of which are used to search for transiting exoplanets while the others are dedicated to asteroseismology (Moutou, 2006). With CoRoT it is now possible to observe a field continuously for approx. 150 days making

it possible to detect planets with long periods (Boisnard et al., 2006). At the time of writing, there have been seven planets published, with one being the first transiting Super-Earth (Leger et al., 2009).

Kepler Launched in 2009, the Kepler satellite is the latest-generation planet detection and asteroseismology satellite. It has an aperture of 0.95 m and a field of view of 105deg^2 and has proven to be capable of achieving the photometric precision necessary to detect Earth-like planets (Borucki et al., 2009). Kepler is located in an Earth-trailing heliocentric orbit and observes each field for 3 consecutive months aiming to detect Earth-sized objects.

1.2.2 The Transiting Exoplanet Sample

Here, I will briefly describe the properties of the sample of transiting exoplanets. Since there is no reason why planetary systems with orbits which are not aligned edge-on should be intrinsically different, the characteristics determined for transiting planets have great value for the study of planets in general.

Many Hot and some Bloated Jupiters

In Figure 1.4, the mass of the transiting exoplanets is plotted versus their semi-major axis and one can distinguish that, with a few exceptions which will be discussed below, all planets can be considered Hot Jupiters.

When the first known transiting exoplanet, HD 209458 was discovered, its mean density was calculated to be $0.31 \pm 0.07 \text{ g cm}^{-3}$, proving its nature as a gas giant (Charbonneau et al., 2000). As a model for this planet was devised by Burrows et al. (2000), it was clear that the radius was larger than expected for a “cold” gas giant, a trait which turned out to be shared by many of the planets discovered in the following years (a comprehensive overview on transiting planet parameters can be found in Torres et al. 2008). The reason for these large radii is yet unclear, and it is likely that more than one mechanism is responsible and that the mechanisms work with different strengths in different systems. The most straight-forward explanation for this bloating of Hot Jupiters is that the atmosphere is irradiated due to the close proximity to the star. An irradiated planet is less effective at disposing of gravo-thermal-energy and thus contracts much more slowly than an isolated planet (Guillot et al., 1996). Still, this hypothesis can not explain the radii of several very bloated exoplanets and thus other mechanisms must be at work. Suggestions for these mechanisms include tidal heating, or the absorption of stellar flux combined with atmospheric circulation (Leconte et al., 2009, and references therein). Naturally, the chemical composition of the planet also plays a crucial role. While many exoplanets show large radii and thus small densities, there are a few cases of planets which are known to be massive but compact, with very massive cores. As an example, HD 149026 (orbiting at $a = 0.04 \text{ AU}$) has an inferred core mass of approx. $67 M_{\oplus}$ (Sato et al., 2005) while its total mass $0.359 \pm 0.022 M_J$ is close to that of Saturn (Torres et al., 2008). Another object, CoRoT-3, has a mass of

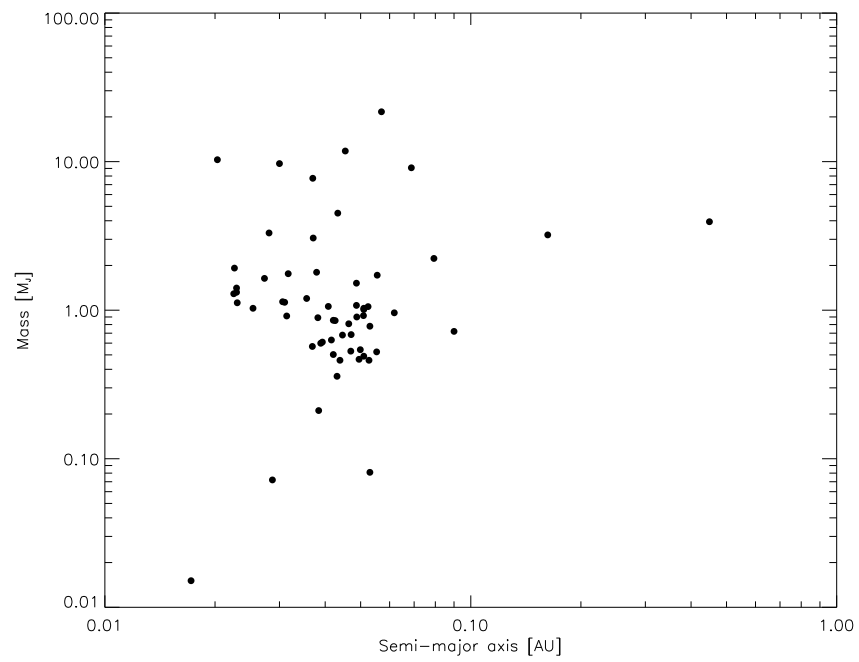


Figure 1.4: The a - M diagram of the transiting exoplanets known up to date. Clearly, the bulk of the discoveries are located at small orbital separations and have masses similar to that of Jupiter.

approx. $21.66 \pm 1.0 M_J$ while having a radius of $1.01 \pm 0.07 R_J$ producing a density of $26.4 \pm 5.6 \text{ g cm}^{-3}$. It is reasonable to assume that this object belongs to the class of brown dwarfs.

Two Hot Neptunes and One Hot Super-Earth

Towards the low-mass regime, only three discoveries have been made among transiting planets, namely the Hot Neptunes GJ 436 b (discovered by Butler et al. (2004), transits detected by Gillon et al. (2007)) and HAT-P-11 b (Bakos et al., 2009c) together with CoRoT's first discovery in the low mass range, the Hot Super-Earth CoRoT-7 b (Leger et al., 2009). While little is known yet about the latter two planets, GJ 436 has been studied to great extent. Summarizing the discoveries regarding GJ 436, which orbits an M-dwarf producing pronounced transit and radial-velocity signatures, one should mention that irregularities have been detected in its mid-transit times but so far, no additional planet in the GJ 436 system could be confidently identified (Ballard et al., 2009, and references therein). GJ 436 b is believed to be more "rocky" than Neptune, but no "Super-Earth" being composed of between 5% and 30% Hydrogen and Helium and less than 90% rock and iron (Figueira et al., 2009).

1.2.3 Other Properties Accessible for Transiting Exoplanets

Not only does the transit itself offer a possibility to determine the fundamental properties of the planet, e.g. its true mass and mean density, the fact that transiting planets pass between us and the host star allows us to measure a number of additional quantities. As already described in section 1.1.5, the detection of chemical elements in exoplanet atmospheres is possible with photometry or spectroscopy in the infrared. But also with optical photometry, the planetary albedo can be estimated from variation of the out-of-transit light curve which is correlated with the planetary phase, and from the depth of the secondary eclipse (e.g. Rowe et al., 2008). Simply knowing the location of the secondary eclipse allows us to evaluate the eccentricity of the orbit. In the light of planet formation scenarios, it is interesting to know the orientation of the planetary orbit with reference to the stellar spin, a quantity which can be derived with help of the *Rossiter McLaughlin Effect*. The Rossiter-McLaughlin Effect occurs when an opaque object passes in front of a rotating star, occulting part of the rotating disk and thus decreasing the amount of light coming from that part of the star. If the planet covers a region of the star which has a positive (negative) radial velocity the overall measurement of the radial velocity will decrease (increase). From the shape of this variation, the spin-orbit angle can be inferred (Queloz et al., 2000). Last but not least, the transit light curves give good measurements of the planetary period, and provided one has a sufficiently large dataset, variations in the planetary period which can be attributed to perturbing bodies such as exomoons, Trojans or additional planets can be identified. This technique is called *Transit Timing* and will be discussed in

detail in chapter 2.

1.3 Layout of the Thesis

The aim of this work is to probe a planetary system, OGLE2-TR-L9 for transit timing variations. For this purpose, five new transits were recorded at the 2.2m MPI/ESO telescope at La Silla observatory. The observed transits are then used to find improved parameters of the OGLE2-TR-L9 system and search for irregularities in the planetary period.

The subject of this work, OGLE2-TR-L9 b was initially identified as a planetary candidate in the publicly available dataset of the OGLE-II survey which was aimed at discovering microlensing events in the galactic bulge (Udalski et al., 1997) by Snellen et al. (2007). It was confirmed as a transiting exoplanet by Snellen et al. (2009) with the observation of a full transit and radial velocity measurements. With a mass of $4.5 \pm 1.5 M_J$ and a period of approximately 2.5 days, OGLE2-TR-L9 b orbits an F3V star, one of the hottest stars known to host a transiting planet.

This work is structured as follows: in chapter 2, I will elaborate on the transit timing technique, followed by an detailed description of the observation and data reduction process in chapter 3. In chapter 4, I will present the model for a planetary transit and discuss the fitting process. In chapter 5, the results with regard to planetary parameters and transit timing will be discussed. Finally, a summary of the performed work will be given in chapter 6.

Chapter 2

The Transit Timing Variations Technique

In this chapter, a short introduction to the transit timing variations technique will be given. While the general concept will be introduced in section 2.1, a short summary of transit timing studies performed so far will be given in section 2.2 and the future perspectives in the light of new discoveries will be described in section 2.3.

2.1 The Transit Timing Method

As described in the section 1.2.2, almost all transiting exoplanets are giants located at very small orbital separations, a property which is mainly due to the detection biases applying to the transit method. There is, however, no reason to believe that there are no further-out objects present in these systems, especially objects with masses small enough to elude detection via radial velocity measurements. Although their detection can be extremely difficult with traditional methods, their gravitational impact on the transiting planet's orbit can be measured as dynamical interactions within the system cause the period of the transiting planet to vary and in turn, the transit occurs earlier or later than expected (Holman and Murray, 2005). The Transit Timing Method aims at discovering additional planets by searching for changes in the mid-transit times of close-in transiting exoplanets. Naturally, this technique is more sensitive to massive perturbers but for planets located near mean motion resonances with the transiting giant, it can be sensitive enough to detect planets of a few Earth masses. Figure 2.1, which is taken from Agol et al. (2005) illustrates the above fact depicting the sensitivity of the transit timing method in comparison to the radial-velocity and astrometry methods for the HD 209548 system. The scenario of smaller planets located in mean-motion resonances is, according to models of planet formation and migration (Thommes, 2005; Papaloizou, 2005), quite likely.

An estimate of the magnitude of the timing variation expected is given by Agol et al. (2005). For a perturber in the outer 1:2 resonance, the maximum O-C residual

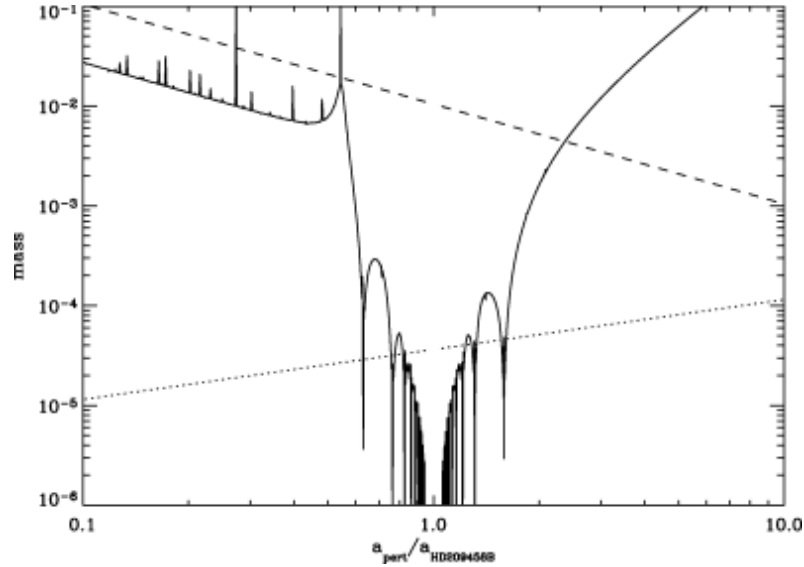


Figure 2.1: In this Figure, taken from Agol et al. (2005), the sensitivities of the transit timing (continuous line), radial-velocity (dotted line) and astrometric (dashed line) planet detection methods are depicted for the HD 209458 - system. The mass is given in solar masses, while the semi-major axis is given in units of the semi-major axis of the Hot Jupiter HD 209458 b. While the sensitivity of the radial-velocity method increases linearly, the transit timing technique peaks in efficiency at the mean-motion resonances.

is:

$$\delta t_{max} = \frac{P}{4.5} \frac{m_{pert}}{m_{pert} + m_{trans}} \quad (2.1)$$

Applying this formula to OGLE2-TR-L9, for perturbers with $1 M_{\oplus}$ and $2 M_{\oplus}$, we get estimated perturbations of 33s and 66s respectively. With the transit timing method, not only additional planets can be detected, it is also possible to measure the effects caused by a moon (Kipping, 2009) or a Trojan of the transiting planet (Ford and Holman, 2007). Calculated timing variations for various perturbers are shown in Figure 2.2.

Apart from transit timing variations, some configurations can also cause variations of the transit duration. These can be due to either a change of the orbital speed caused by an exomoon (Kipping, 2009) or due to a change in the inclination, as was believed to be the case for GJ 436 b (Ribas et al., 2008). Here, the inclination of GJ 436 b was believed to increase due to an interior $5M_{\oplus}$ perturber and so the transit could not be detected in earlier observations. The existence of this planet has, however, been ruled out by subsequent studies (Bean and Seifahrt, 2008). Still, precise measurements of the transit duration can provide additional

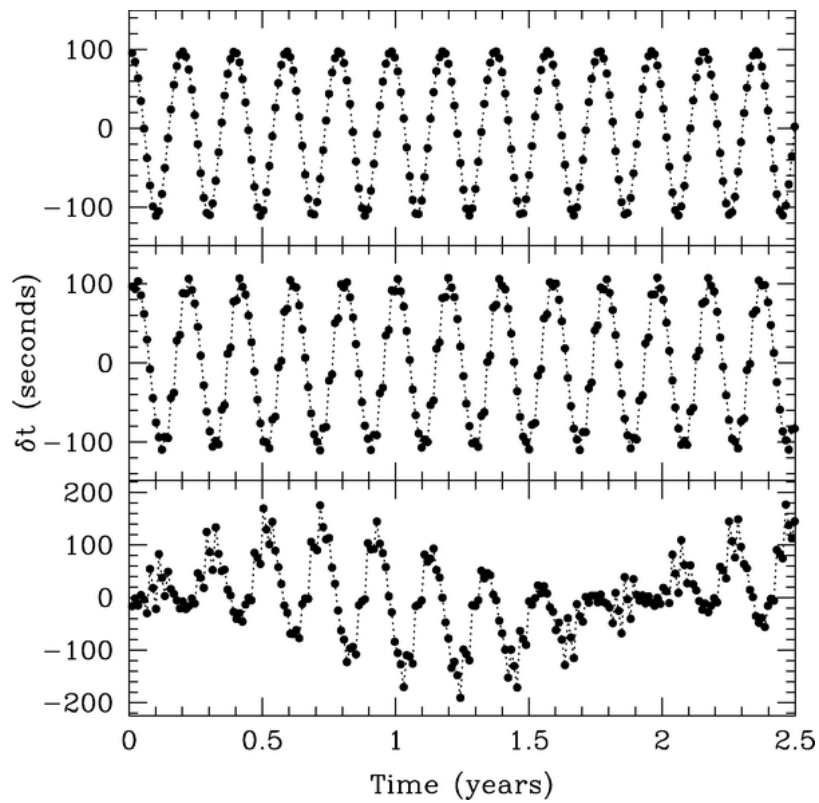


Figure 2.2: Different transit signatures calculated for an Hot Jupiter of $0.5 M_J$ and a period of 4.09 days. The perturbing planet is a $1 M_\oplus$ Trojan in the upper panel, a $28 M_\oplus$ planet with a period of ~ 8.7 days (not in resonance) in the middle panel and a $\sim 4.8 M_\oplus$ planet with a period of ~ 5.91 days (inside the 3 : 2 mean motion resonance) in the lower panel; Ford and Holman (2007).

clues about perturbing bodies in the system. Once hypothetical transit timing variations have been identified, it is necessary to perform three-body simulations for a large variety of configurations to identify the nature of the perturber.

2.2 Results of Previous Searches

At the current point in time, many transiting systems have been probed, at least to a limited extent, for transit timing variations, and although already a considerable amount of time has been invested in the search for transit timing variations there has not yet been a conclusive detection. While some systems do not show any indications for transit timing variations (e.g. Corot-1 (Bean, 2009), Corot-2 (Alonso et al., 2009) and HD 209458 (Miller-Ricci et al., 2008)), the mid-transit times measured for some other systems do not seem to agree with a constant period (e.g. OGLE-TR-111 (Díaz et al., 2008) and HD 149026 (Carter et al., 2009)). For the latter group of planetary systems, it is yet unclear whether the observed O-C distribution is due to actual transit timing variations or whether it is an artifact of observational uncertainties which have been underestimated. There are two systems which deserve special interest:

GJ 436 After the planet GJ 436 b was shown to transit by Gillon et al. (2007), it has been repeatedly studied for transit timing variations as it is a promising target due to its non-zero eccentricity and its small mass. While Ribas et al. (2008) proposed a perturber interior to GJ 436 b on the basis of radial-velocity measurements together with a putative change in inclination, the analysis of additional data by Alonso et al. (2008) and Ribas et al. (2008) forced a retraction of planet c. Still, the new observations do not refute the existence of an additional planet in the GJ 436 system and further transits have been observed (Ballard et al., 2009; Caceres et al., 2009; Shporer et al., 2009; Bean et al., 2008; Coughlin et al., 2008; Stringfellow et al., 2009) providing a set of new transit timings which are indicative of some parameter variations in GJ 436 b. Figure 2.3, taken from Caceres et al. (2009) shows an O-C diagram for the observed mid-transit times.

HD 17156 For the system HD 17156, recently a second planet was announced by Welsh (2009) on the basis of transit timing variations. At the time of writing, no details have yet been published about this discovery so it remains to be seen whether it will hold up to independent confirmation.

2.3 Future Perspectives

The performance of the transit timing technique strongly depends on the availability and quality of as many mid-transit measurements as possible. Photometry satellites provide a long time baseline and coverage of a large number of transits and thus datasets which are ideal for the study for transit timing variations. While

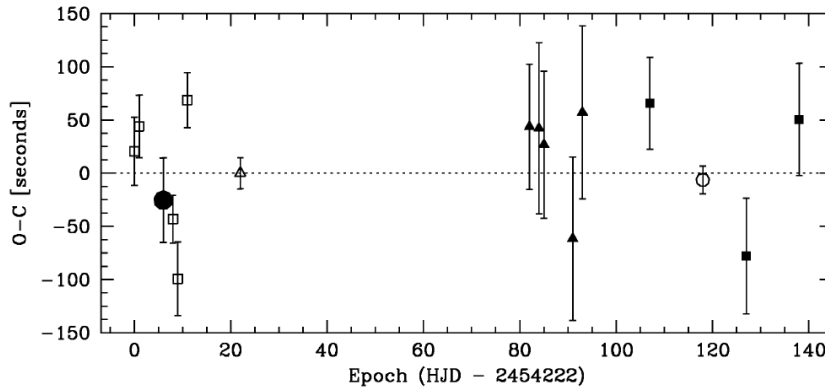


Figure 2.3: Here the O-C diagram for GJ 436 is depicted, showing that the mid-transit times seem to vary from a constant period. The symbols refer to different literature sources; Caceres et al. (2009)

some CoRoT data already has been searched for transit timing variations (Bean, 2009), the Kepler satellite has only been operational for a short period of time. Given the high accuracy of the Kepler photometry (Borucki et al., 2009), it can be assumed that the mid-transit time measurements are very exact and we can expect some high accuracy transit timing studies. A detailed analysis of the potential to discover low mass objects with Kepler is given in Kipping (2009).

Another interesting test of the transit timing technique will be the study of the newly discovered planet HAT-P-13, which hosts a massive ($M=15.2 \pm 1 M_J$, $P = 428.5 \pm 3 d$) exterior companion together with a transiting Hot Jupiter (Bakos et al., 2009b). While currently there are not yet enough good quality data available, we will soon be able to judge whether the transit timing technique would have been able to identify HAT-P-13 c.

Chapter 3

Observations and Data Reduction

In this chapter, I describe the steps necessary in the process of observing and analyzing photometry of planetary transits.

In section 3.1, the observing process, starting from choosing target, instrument and telescope to the on-site observing procedures which I used to increase data quality are described. Clearly, there are always unforeseen difficulties and problems incurred in the course of an observing run.

In section 3.2, I will focus on the actual data reduction process. I will provide a description of the reduction methods used to obtain a light curve from photometric measurements and describe the programs developed to perform differential photometry. At the end of section 3.2 the produced light curves are presented.

3.1 Observations

3.1.1 Target and Site Selection

The selection of OGLE2-TR-L9 as a target for the observations was based largely on reasons such as observing time availability and visibility of the target. For the observations we aimed at the guaranteed-time periods of the Max Planck Institute for Extraterrestrial Physics and the Max Planck Institute for Astronomy during April 2009. During this period, we had the chance to observe four transits of OGLE2-TR-L9. An additional transit was observed during May. Even disregarding the hope to detect transit timing variations, OGLE2-TR-L9 is a rewarding target since it is nearly unstudied (it had only one transit recorded in the past) and being an F3V star makes it the hottest star with a known transiting companion (Snellen et al., 2009). Additionally, with a magnitude of $I = 13.94$ it is the brightest planet host star discovered from the OGLE sample allowing the exposure time to be kept reasonably short.

The instrument of choice, GROND (Gamma Ray Burst Optical and Near-Infrared Detector) is a 7 channel imager designed to observe gamma-ray-burst afterglows (Greiner et al., 2008) which is mounted at the MPI/ESO 2.2m telescope

Start Time [UT]	End Time [UT]	Observer(s)
2009 04 11, 03:09	2009 04 11, 07:37	J. Koppenhoefer
2009 04 16, 03:12	2009 04 16, 07:28	J. Koppenhoefer, M. Lendl
2009 04 21, 02:03	2009 04 21, 06:00	M. Lendl
2009 04 26, 01:29	2009 04 26, 05:29	M. Lendl
2009 05 15, 23:13	2009 05 16, 02:58	A. Rossi

Table 3.1: This table summarizes the exact observing times and observers on site

at La Silla observatory. It simultaneously observes in 4 optical ($g' r' i' z'$) and 3 infrared ($J H K$) channels allowing to gather multicolor observations of each transit. Since the infrared data are limited to an exposure time of 10s and thus not have sufficient signal to noise to detect the transit, the focus of this work lies on the optical data.

3.1.2 Observation Strategy

The observations took place on April 10, 15, 20, 25 and May 15 2009, corresponding to the Epochs 177, 179, 181, 183 and 191 based on the ephemeris given by Snellen et al. (2009). During each night, we observed the full transit plus at least 20 minutes of baseline before ingress and after egress which is important to derive a good out-of-transit magnitude of the star. A detailed list of the observation times and observers is given in table 3.1. For all observations, the exposure time was kept fixed at 46.4 s. There are a few settings which the observer has to choose:

Dithering The default mode for observations with GROND is to follow a dithering pattern of four positions. I would, however, like to note that for time-series photometry this is not the optimal choice, it decreases the cadence and introduces photometric variations which are due to the different sensitivity levels on the CCD. Consequently, during my observations, I used no dithering.

Read-out GROND has two read-out modes available, the slow (standard) readout mode of (~ 45 s) and the fast (~ 15 s) readout mode. It comes without saying that for time-series-photometry, which has the purpose of collecting as many images as possible, the fast readout mode is the preferred choice.

3.1.3 Observing Process

During the night of April 10 (UT), the slow (~ 45 s) readout mode was used in combination with the standard dithering pattern of four positions achieving a cadence of 2.05 minutes. The seeing ranged from 0.87'' to 1.8'' while the airmass was between 1.19 and 1.90 during the observation. We incurred some problems with guiding during the night of April 15 (UT), leading to the stars having elongated

Evening Date	g'-filter	r'-filter	i'-filter	z'-filter
2009 04 10	1.73	1.42	1.89	1.76
2009 04 15	1.63	1.39	1.78	1.68
2009 04 20	1.38	1.17	1.71	1.62
2009 04 25	1.29	0.97	1.45	1.79
2009 05 15	1.35	1.18	1.66	1.90

Table 3.2: The RMS scatter [mmag] in the data for each filter during and night. Note that the r'-filter has the lowest scatter.

shapes on some pictures; especially in the first half hour the guiding repeatedly went off track during its readout. We managed to keep the problems under control by selecting a bright guide star and thus short cycle rates on the guider. Switching from 4-position-dithering to no dithering after 20 exposures also helped to limit the effects of the problem since there was no more need to change the guide star after each exposure. During this night, we observed with an average cadence of 1.95 minutes and covered air masses from 1.20 to 1.96 while the seeing ranged from 0.7 to 1.2". For the nights of April 20, 25 and May 15 (UT), we used the fast readout mode together with no dithering, increasing the cadence to 1.31 minutes for April 20 and 1.25 minutes for April 25 and May 15. The observations took place at air masses from 1.18 to 1.60, 1.18 to 1.55 and 1.18 to 1.34 for these three dates, respectively while the seeing ranged from 0.5" to 1.1" for April 20 and 0.5" to 0.9" for April 25. The above values for the seeing refer to the DIMM instrument at La Silla observatory which was not operative on May 15 2009. For May 15, the seeing estimated from the observations ranges from 0.5" to 0.9". In our analysis, we included the transit observed with GROND on January 27 (UT), 2008. The observation procedure was essentially the same as in the April 10 observation, a detailed description can be found in Snellen et al. (2009).

Comparing the data obtained with the slow readout mode and dithering to the data obtained with the fast readout mode and without dithering, it shows that the adapted observation procedure indeed improved the data quality, increasing the cadence by a factor of 1.5 and decreasing the scatter of the RMS residuals from 1.42 mmag to 1.1 mmag. A summary of the RMS scatters for all nights and filters can be found in table 3.2.

3.2 Data Reduction

It is, since the purpose of the initial OGLE observations was to detect microlensing events, not surprising that OGLE-TR-L9 is located in a rather crowded field. Fortunately, OGLE2-TR-L9 is fairly isolated (see Figure 3.1 for a finding chart), with only very minor sources in its vicinity allowing the use of aperture photometry. There is a variety of programs one can use to produce light curves with aperture

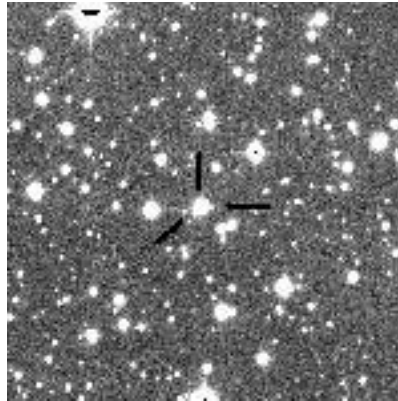


Figure 3.1: Finding chart for OGLE2-TR-L9, note the crowdedness of the field and the minor sources located next to the target.

photometry. In this work, I have used two of them, the *mupipe* software, which is developed at the University Observatory Munich¹, and IRAF² daophot and compared the results.

3.2.1 Basic Image Reduction

First of all, it is necessary to remove systematic effects from the images that contain the scientific data. Therefore, several correction procedures have to be applied:

Overscan On many CCDs, there is a strip of pixels which are not exposed to light. This strip can serve as a measure for the dark and bias levels during the night. The usual procedure is to subtract an average overscan value from all pixels in the image.

Bias The bias is often referred to as the initial offset of a pixel independent of the amount of light captured. It can be illustrated by the following example: provided we would readout a CCD which has not been exposed to any light source and with an exposure time of 0 seconds, we would expect all pixel values to be equal to zero. In reality, however, due to some intrinsic charges in the pixel together with readout noise, the values will be small but positive. A way to compensate for this offset is to take a number of frames with minimal exposure time and closed shutter, combine them to a master-frame and subtract the values pixel-by-pixel from the science frames.

¹*mupipe* is available from <http://www.usm.uni-muenchen.de/people/arri/mupipe/>

²IRAF is distributed by the National Optical Astronomy Observatories, which are operated by the Association of Universities for Research in Astronomy, Inc., under cooperative agreement with the National Science Foundation.

Dark When taking frames with non-zero exposure times, we also have to take into account the noise created by the thermal movement within the pixels due to which electrons are released mimicking the effect of infalling photons. Naturally, the amount of “dark current” depends linearly on the exposure time and becomes minimal for very well cooled CCDs.

Flatfield Once the above corrections are done, it is still necessary to compensate for pixel-to-pixel sensitivity variations. For this purpose, an evenly illuminated surface (e.g. the twilight sky) is observed and a normalized master-flat is created. The pixels on the science frames are then weighted by dividing the picture by the master-flat.

3.2.2 Instrument-Specific Image Correction

GRONDS four optical channels possess backside illuminated CCDs with a field-of-view of $5.4\text{arcmin} \times 5.4\text{arcmin}$ (Greiner et al., 2008). Two halves of the CCD are read out simultaneously to save time but leading to two different gain levels which have to be compensated. Both areas have an overscan strip attached. Dark current is minimal for GROND and thus can be neglected in the image correction. For the image correction, the following steps are performed on science and flat images using routines implemented in *mupipe*:

1. The image is split according to the two readout strips.
2. The average overscan is calculated from both regions and is subtracted from the corresponding image areas, ADU are converted to electron values.
3. The two parts are combined to form one image.

Then, discarding flatfield images with bad quality, a masterflat is created and the science frames are divided by it.

3.2.3 Aperture Photometry with IRAF and Manual Creation of a Reference Source

To confirm the light curve obtained with *mupipe* (see section 3.2.4), I performed aperture photometry with the IRAF daophot procedure *phot*. The first step was to align all images of one night and filter on a common grid which was done using the IRAF procedure *imalign*. As a reference image served the image with the smallest FWHM. Then I performed photometry with *phot* for essentially all well resolved and bright stars in the field. The photometry was done for several apertures, ranging from 11 to 14 pixels in order to find the aperture producing the best results. It was found to be 12 pixels. The sky was determined in an annulus from 22 – 32 pixels for all nights apart from May 15 where I used 20 – 30 pixels in order to stay on the same read-out strip.

In order to perform differential photometry, I used *txdump* to collect all the values and errors in one file and transfer them to IDL routines made for the purpose of differential photometry. Then, I iteratively selected approximately 15 of the most stable stars in the field (with the exact number depending on the filter and seeing conditions) and combined them to a reference source by weighing them according to the shown scatter. The IDL programs created are:

dumpextract The *dumpextract* routine has the simple purpose of reading the data produced by IRAF and sorting it. For each star, a file called "star_n_red.dat" is created containing the time (t_i), magnitude (mag_{i_n}) and error (err_{i_n}) values.

differenzen The routine *differenzen* reads the files created by *dumpextract*, calculates the Heliocentric Julian Date (HJD_i) from the telescope timestamps and calculates

$$diff_{i_{nm}} = mag_{i_n} - mag_{i_m} \quad (3.1)$$

for all combinations of stars (n,m). It then produces a file for each combination "diff_n-m.dat" containing HJD_i and $diff_{i_{nm}}$ as well as a file for each star "star_nHJD.dat" containing the HJD_i , mag_{i_n} and error err_{i_n} values.

refstar *refstar* combines a subset of the stars in order to produce a more stable reference source. The choice of the reference stars is usually based on the curves produced with *differenzen* and iterated until the best combination is found. To produce the reference source, *refstar* reads all the "star_nHJD.dat" - files together with the measurements of the target. The scatter (σ_n) in the measurements of each star is calculated and then the weighting factors ($factor_n$) are calculated via

$$factor_n = \left[\frac{\frac{1}{N} \sum_{j=1}^n \sigma_j}{\sigma_n} \right]^2 \quad (3.2)$$

where N is the total number of reference stars included. To calculate the magnitude-values of the reference source ($mag_{i_{ref}}$) and the corresponding errors ($err_{i_{ref}}$), first two arrays are created:

$$wertearray = \begin{pmatrix} mag_{1_1} & mag_{1_2} & \dots \\ mag_{2_1} & mag_{2_2} & \dots \\ \vdots & \vdots & \ddots \end{pmatrix} \quad (3.3)$$

and

$$errorarray = \begin{pmatrix} (err_{1_1})^2 & (err_{1_2})^2 & \dots \\ (err_{2_1})^2 & (err_{2_2})^2 & \dots \\ \vdots & \vdots & \ddots \end{pmatrix}. \quad (3.4)$$

Together with

$$faktor = \begin{pmatrix} faktor_1 \\ faktor_2 \\ \vdots \end{pmatrix} \quad \text{and} \quad faktor_2 = \begin{pmatrix} (faktor_1)^2 \\ (faktor_2)^2 \\ \vdots \end{pmatrix}, \quad (3.5)$$

we can calculate $(mag_{i_{ref}})$ and $(err_{i_{ref}})$ by

$$(mag_{i_{ref}}) = wertearray \cdot faktor \quad (3.6)$$

and

$$(err_{i_{ref}}) = \frac{1}{N} (errorarray \cdot faktor_2)^{\frac{1}{2}}. \quad (3.7)$$

Finally, the above calculated values of the reference source are subtracted from the measurements of OGLE2-TR-L9 and thus a light curve is created.

3.2.4 Aperture Photometry with *mupipe*

The *mupipe* software which is developed at the University Observatory Munich is able to perform aperture photometry including full error propagation with the routine *refstar*. However, it requires the images to be aligned with a very high accuracy, so I used the IRAF procedure *imalign* to align the pictures on a common reference grid. Two iterations were necessary to achieve an alignment on the 0.1 pixel - scale. The aperture radii were chosen ranging from 11 – 14 pixels (as for IRAF, 12 turned out to produce the best results) and the background level was determined in an annulus from 22 – 32 pixels. The reference stars were chosen, for comparison purposes, identical to the reference stars used with IRAF.

3.2.5 Comparison

Comparing the IRAF-reduced light curves of the r' filter to the light curves produced with *mupipe*, it turns out that the light curves produced with IRAF show smaller scatter. Therefore only the light curves produced with IRAF were used for the analysis. Comparing the light curves in the four optical channels, the light curve obtained in the r' filter shows the least scatter, with an rms scatter of the photometric residuals (see section 4.1 for details on the fit) of 1.25 mmag, considerably lower than 1.48 mmag, 1.70 mmag and 1.75 mmag for the g', i' and z' channels respectively. The quality of the photometry for all nights and channels is collected in table 3.2. All light curves are presented in Figures 3.2 - 3.6.

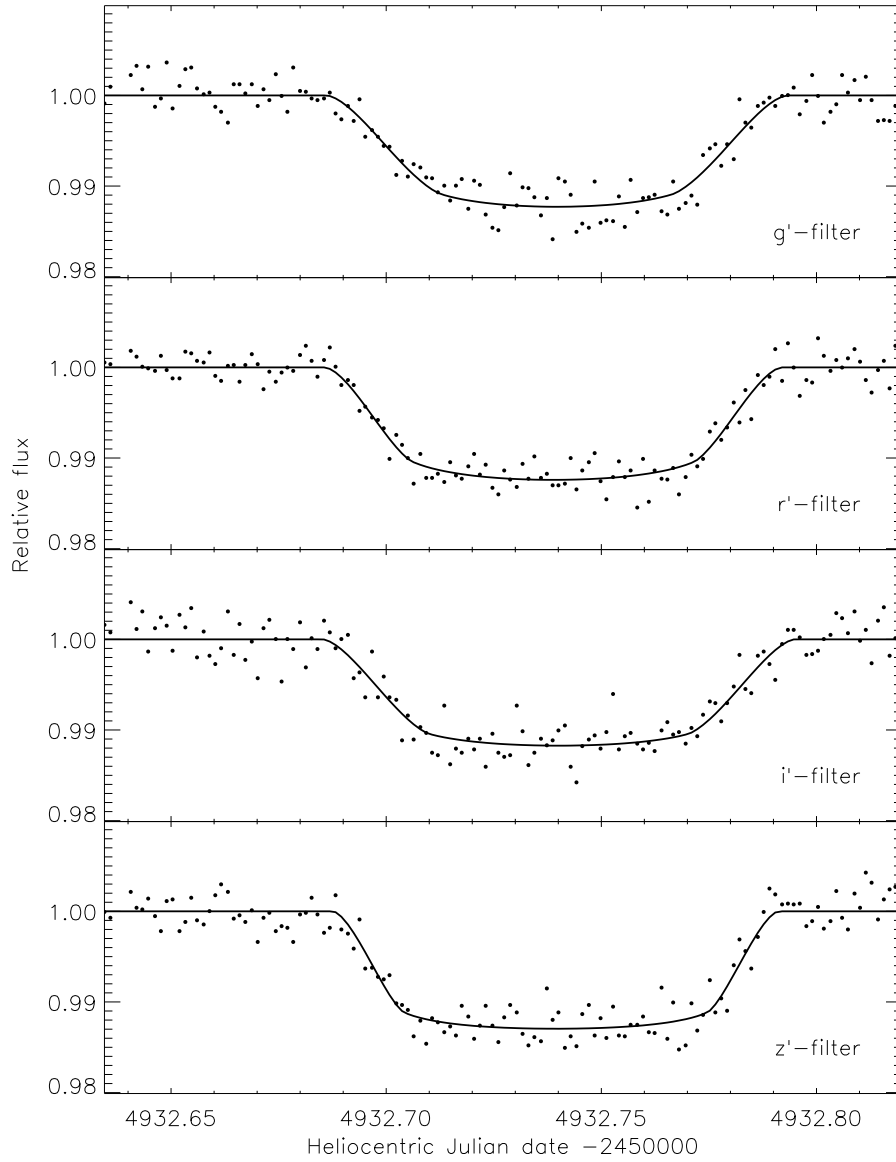


Figure 3.2: The transit of OGLE2-TR-L9 recorded during the night of April 10, 2009 in the four optical GROND channels.

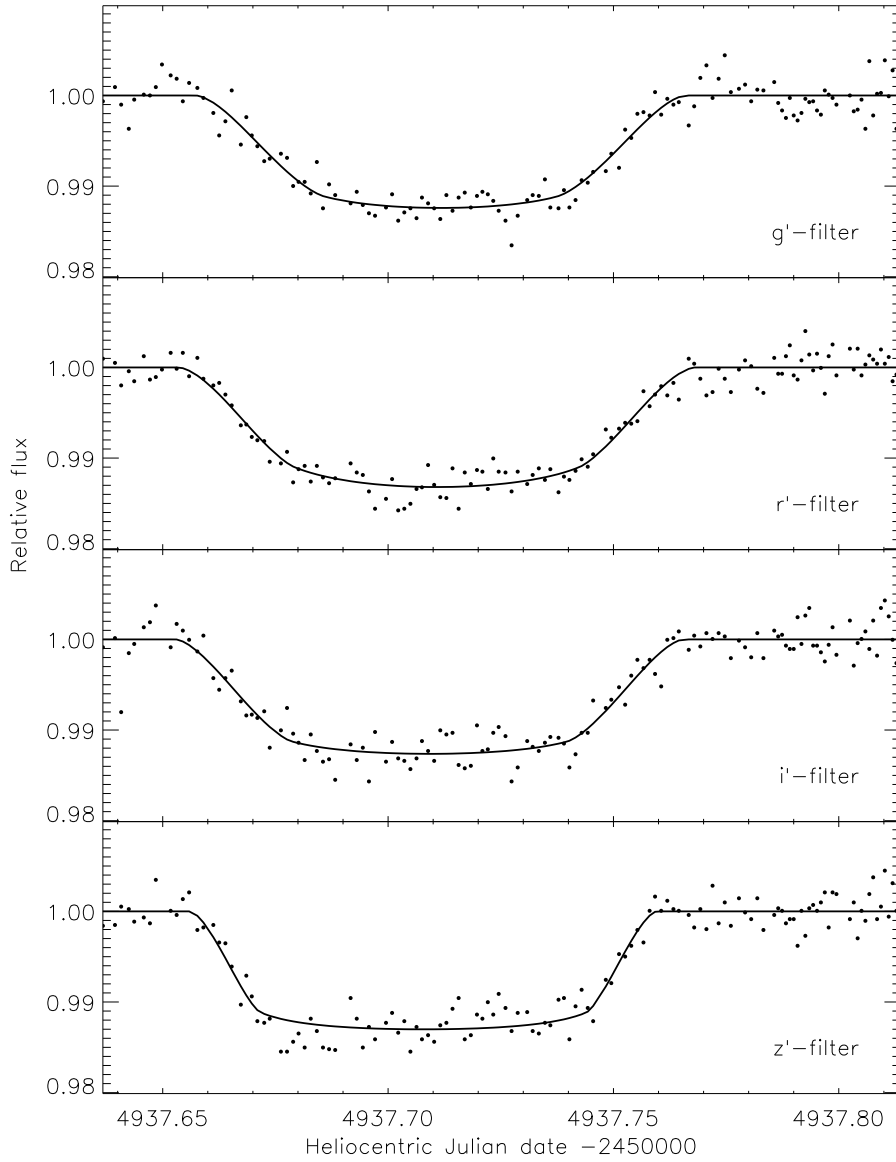


Figure 3.3: The transit of OGLE2-TR-L9 recorded during the night of April 15, 2009 in the four optical GROND channels.

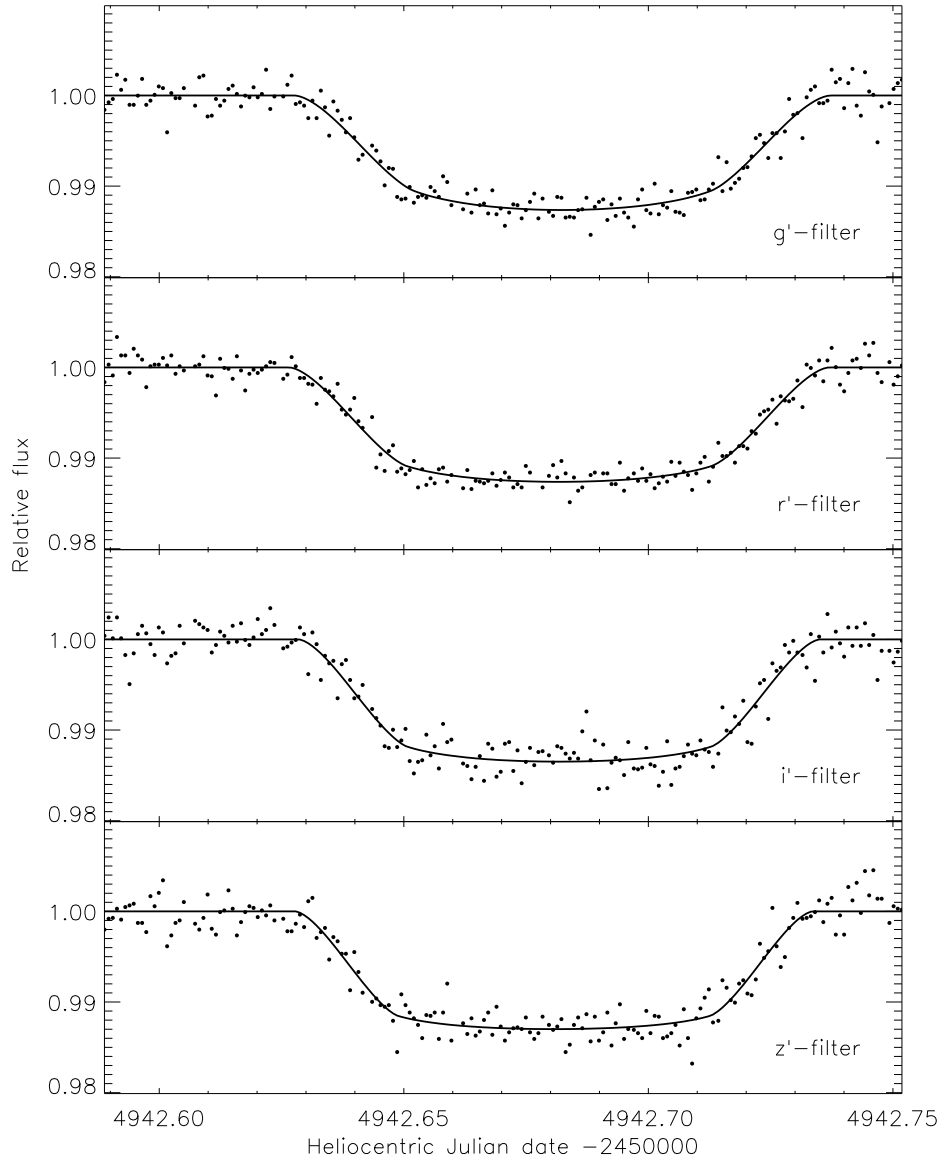


Figure 3.4: The transit of OGLE2-TR-L9 recorded during the night of April 20, 2009 in the four optical GROND channels.

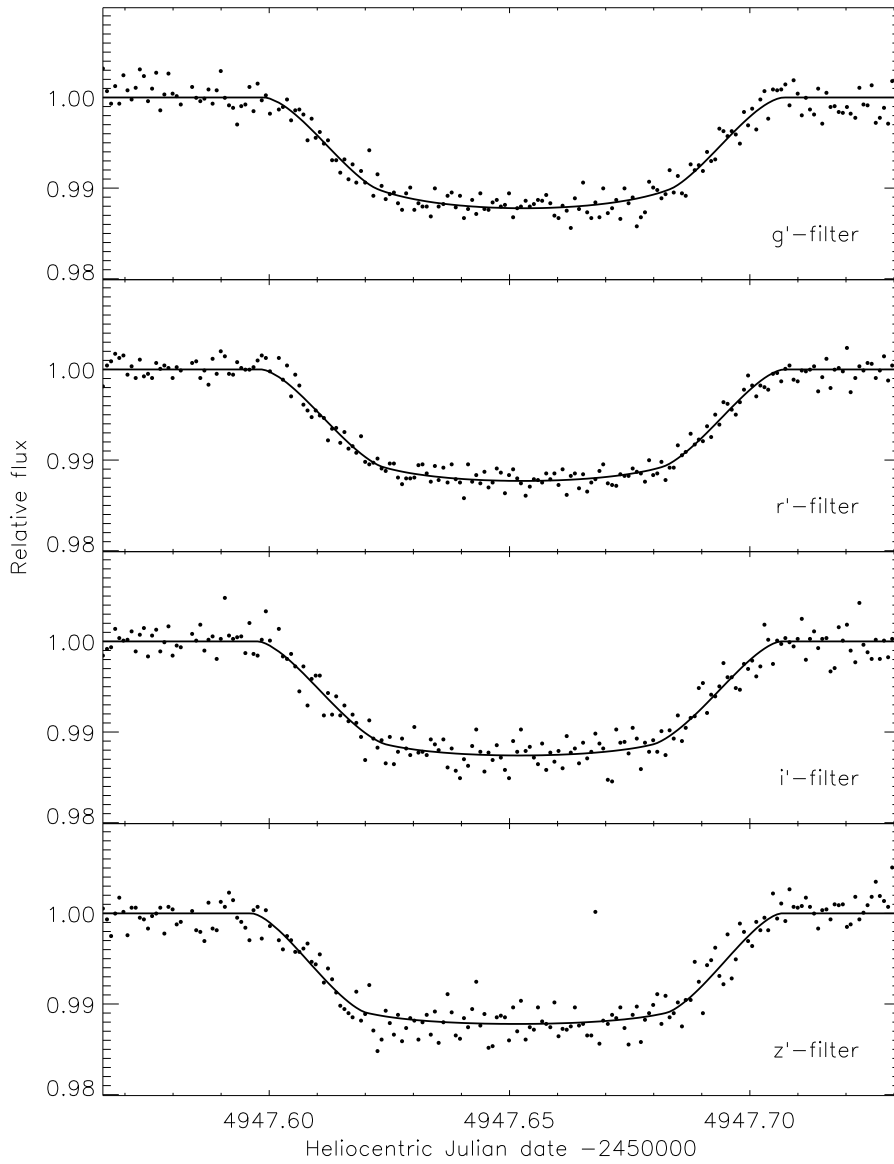


Figure 3.5: The transit of OGLE2-TR-L9 recorded during the night of April 25, 2009 in the four optical GROND channels.

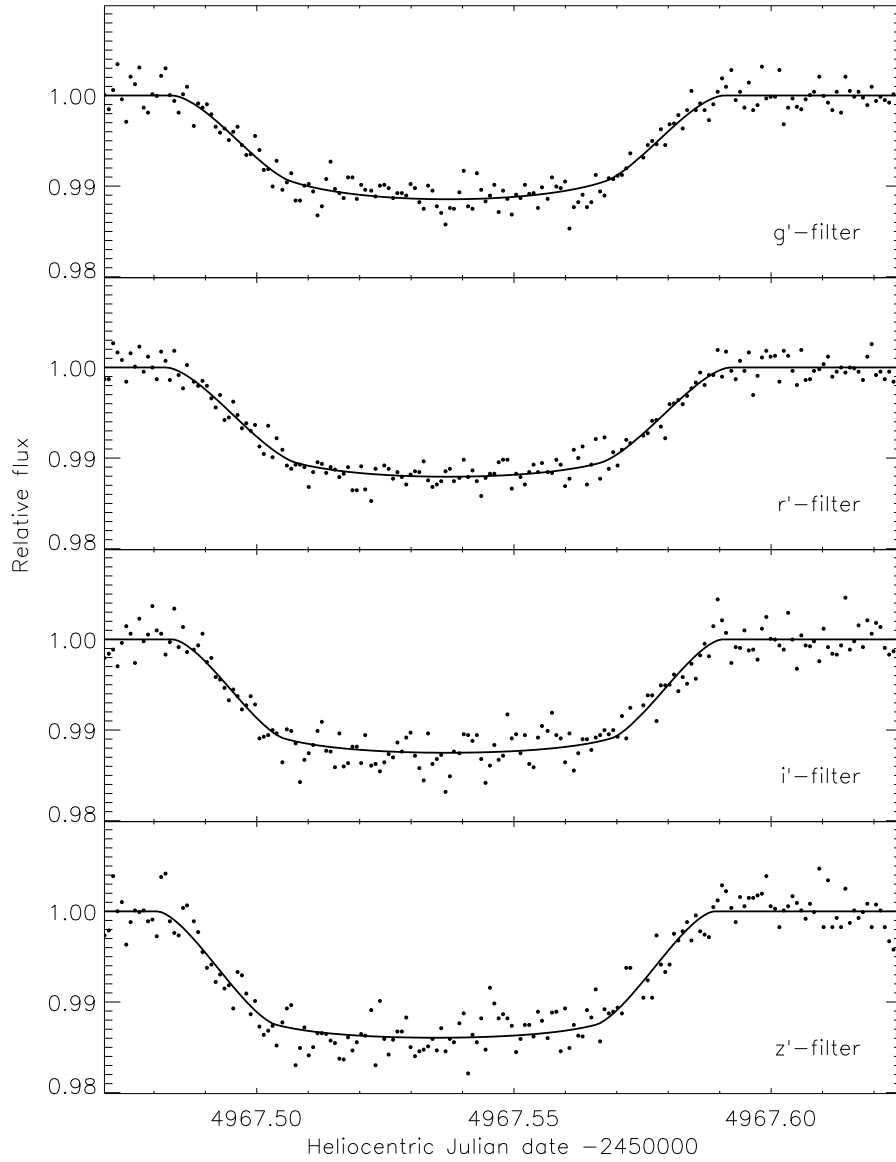


Figure 3.6: The transit of OGLE2-TR-L9 recorded during the night of May 15, 2009 in the four optical GROND channels.

Chapter 4

Determination of System Parameters

Once the transit light curves have been produced, we can use them to find the parameters of the planet.

The basic but less accurate way to do so is to calculate the planetary parameters directly from features of the light curve, such as the depth, the time spent in ingress or egress and, if measured, the period. This way, one finds a fast solution, but does not take into account effects such as the limb darkening of the star. The more professional way to calculate the planetary parameters is to use a model light curve of a planetary transit which takes all necessary effects into account and vary the parameters until the model best fits the data.

In section 4.1, I will describe the model used together with the unknown parameters and in section 4.2, I will describe the programs developed to find the planetary parameters. Finally, in section 4.3, I will give details on the error calculation.

4.1 The Model

The most basic model of a transit light curve is simple. First, while the planet is next to the star, the total stellar flux is measured, followed by a phase in which the planet gradually moves in front of the star, occulting an increasing fraction of the stellar disk and consequently blocking an increasing fraction of light. While the planet is entirely in front of the star, the planet blocks an amount of light equal to the square of the radii ratio

$$\Delta F = \left(\frac{R_P}{R_*} \right)^2. \quad (4.1)$$

During egress, the brightness increases again until it reaches the un-obscured brightness as the planet moves out of transit.

Naturally, the above description neglects effects necessary to be taken into account to successfully reproduce the transit light curves: the fact that the planet

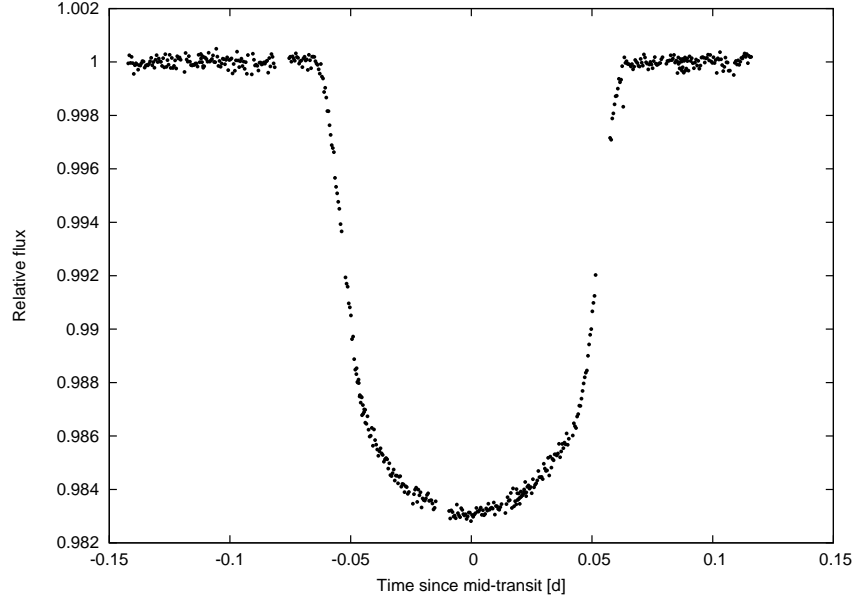


Figure 4.1: A transit of HD 209458 observed by Knutson et al. (2007) with the Hubble Space Telescope. In this high quality light curve, the deviation from a box-like profile caused by stellar limb darkening is clearly visible.

does not pass in front of the star in a straight line and, most importantly, the stellar limb darkening. Stellar limb darkening refers to the effect that the stellar disk appears fainter further away from the center than close to it. This effect is crucial to the correct interpretation of transit light curves at optical wavelengths but has only limited impact towards the infrared. In Figure 4.1, a transit observed with the Hubble Space Telescope STIS instrument at a wavelength of 484 nm is shown. The effect of limb darkening in curving the bottom of the curve is clearly visible (Knutson et al., 2007). To account for limb darkening, I assumed a quadratic limb darkening law,

$$I(r) = 1 - u_1(1 - \mu) - u_2(1 - \mu)^2 \quad (4.2)$$

(where $I(r)$ is the specific intensity and $\mu = \cos(\theta)$ is the cosine of the angle between the observer and the normal to the stellar surface at radius r) and chose the coefficients according to the tables in Claret (2004) for a star with metallicity $[Fe/H] = 0.0$, surface gravity $\log(g) = 4.5$ and effective temperature of $T_{eff} = 7000K$.

In this work, I use the model of a planetary transit given by Mandel and Agol (2002) which works the following way: For each point in time the normalized separation $z = d/r_*$ (d is the projected separation of the planetary and stellar centers) is calculated via

$$z(t) = \frac{a_p}{r_*} \left[(\sin(\omega t))^2 + (\cos(\text{inc}) \cos(\omega t))^2 \right]^{1/2} \quad (4.3)$$

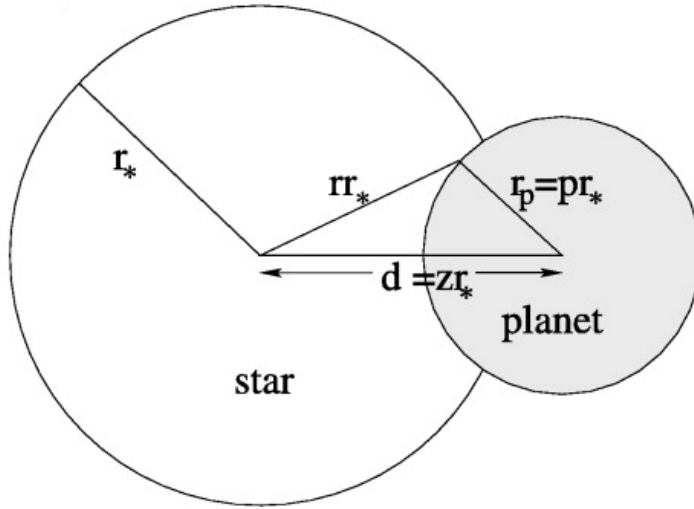


Figure 4.2: Taken from Mandel and Agol (2002), this Figure depicts the geometry of a transit. The parameter z is the projected separation d of the two disk centers divided by the stellar radius.

(here a_p is the orbital separation of the planet, ω is the planet's angular velocity, inc is the inclination and t is the time since mid-transit). The definition of z is depicted in Figure 4.2. Note that $z(t)$ never assumes negative values and only decreases to zero for central transits. Then, together with the radii ratio r_p/r_* , the normalized flux is computed as a function of $z(t)$. This treatment does not account for non-zero eccentricities, which is no problem since OGLE2-TR-L9b has a circular orbit. In total 7 variables, $(a/R_*, r_p/r_*, inc, t_c, \omega = 2\pi/P, u_1, u_2)$ are needed for the model, three of which can be determined by other means: the limb darkening coefficients u_1 and u_2 can be derived from atmospheric models (Claret, 2004) and the angular velocity ω is usually known with sufficient accuracy from previous transit or radial velocity measurements. This leaves us with four values to fit, the normalized semi-major axis a_p/r_* , the radius ratio r_p/r_* , the inclination inc , and the transit midpoint t_c . These parameters have the advantage that they can be derived directly from the light curve without any assumptions regarding stellar properties.

4.2 The Fitting Routine

4.2.1 Overview of the Fitting Process

The best fit to the data was found by minimizing

$$\chi^2 = \sum_{i=1}^N \left[\frac{f_i(\text{obs}) - f_i(\text{calc})}{\sigma_i} \right]^2 \quad (4.4)$$

(where $f_i(\text{obs})$ and $f_i(\text{calc})$ refer to the observed and calculated fluxes at time i and σ_i is the corresponding error) using a downhill simplex algorithm as implemented in the AMOEBA code (Press et al., 1992). As starting values, I first assumed the central transit times calculated according to the ephemeris given by Snellen et al. (2009),

$$T_c(E)[HJD] = 2454492.79765 + 2.4855335E \quad (4.5)$$

and used educated guesses for the other parameters: $r_p/r_* = 0.1$, $a/r_* = 20$ and $inc = 90^\circ$. The fitting routine itself consists of two steps. First I kept t_c fixed and let r_p/r_* , a/r_* and inc vary. Having found the best values, these three parameters were kept fixed and the central transit time t_c was varied. These two steps were iterated three times. After this was done, the light curves for each filter were phase-folded aligning them by the t_c values found. The resulting light curves are shown in Figure 4.3. To refine the parameters once more, I fitted the phased light curves for r_p/r_* , a/r_* and inc , the resulting parameters are shown in table 5.1 and the corresponding model is depicted as a continuous line in Figure 4.3.

4.2.2 The Fitting Programs

The actual fitting process makes use of several IDL routines, partly provided by Mandel and Agol (2002), partly developed newly for this work. Naturally, also the standard IDL routines (for example, *amoeba*) are used. The outline of the fitting process is as follows: first, data and parameters are read by *transitfit* which calls *amoeba* in order to minimize χ^2 . *amoeba* refers to *apimin* and *tmin* where χ^2 is calculated. At each minimization step *apimin* and *tmin* access *occultquad*, a routine provided by Mandel and Agol (2002) to calculate the model light curve for the given parameters. Below, I give a more detailed description of the programs:

transitfit Being provided with the respective transit and planet, *transitfit* starts with reading in dataset (HJD_i , mag_i , err_i) and starting values (a/R_* , r_p/r_* , inc , t_c , ω , u_1 , u_2) for the calculation. It also reads a manually prepared file containing the out-of-transit measurements from which the baseline magnitude (*basemag*) is calculated by taking the average of the out-of-transit values. Next, the values, which are given in magnitudes, need to be converted into relative flux by taking

$$flux_i = 10^{\left(\frac{mag_i - basemag}{2.5}\right)} \quad (4.6)$$

and the *HJD*-values need to be transformed to values reflecting the time since mid-transit by $t_i = HJD_i - t_c$. With all the values accessed and modified by subprograms written into common-blocks, *transitfit* now calls *amoeba* to find the best fit for a/R_* , r_p/r_* and inc . Once the minimization is complete and we have a first guess for the planet's parameters, *amoeba* is called again to find the offset from the actual mid-transit time and the time values are corrected for this offset. With an output after each iteration, the above two

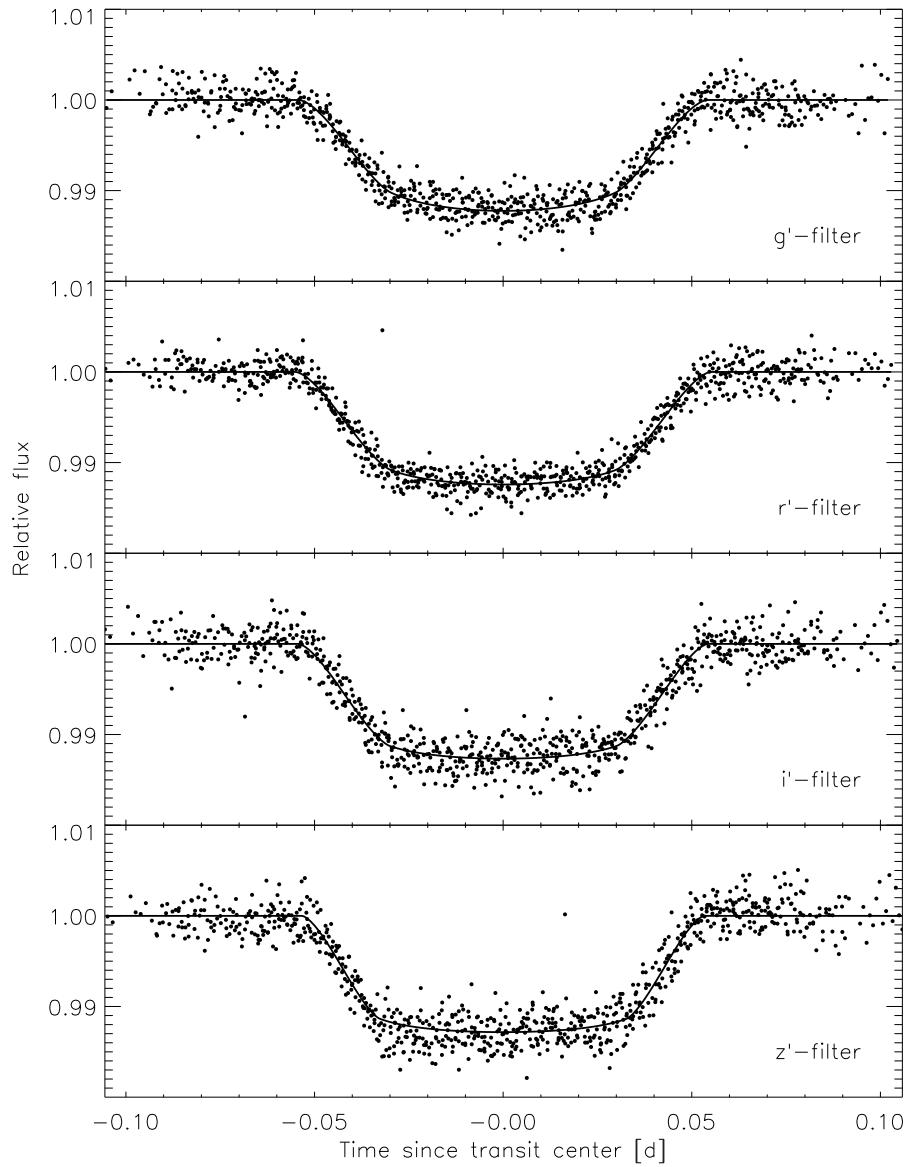


Figure 4.3: The phased light curves of OGLE2-TR-L9. The filters are, from top to bottom: g' , r' , i' and z' . the phased light curve in the r' -filter also contains the new reduction of the data from Snellen et al. (2009). The best fit models are over-plotted as continuous lines.

calls are repeated twice with increasing accuracy. Having found the best values, output files and light curve are created.

amoeba *amoeba* is an IDL implementation of the downhill simplex method for finding the minimum of a function. It needs to be provided with the name of the function which is to be minimized, in this case *apimin* or *tcmim* and starting values.

apimin The function *apimin* has the simple purpose of returning the χ^2 -value given the parameters a/R_* , r_p/r_* and *inc*. It does so by first using equation 4.3 to find the $z(t)$ values from the dataset, then calling *occultquad* to calculate the theoretical flux value for each point and using equation 4.4 to compute the χ^2 of the fit.

tcmim *tcmim* is essentially the same as *apimin*, only it is used when fitting for the transit midpoint.

occultquad Provided by Mandel and Agol (2002), *occultquad* computes a model light curve with quadratic limb darkening. It needs to be provided with the z_i -values (which requires knowledge of a/R_* and *inc*) and r_p/r_* and returns the values of the fit at every point i . For more details, see Mandel and Agol (2002).

4.3 Error Calculation

To estimate the errors of the determined parameters, two complementary methods, the *Bootstrap Monte Carlo* method and the variation of the χ^2 , were used and compared. Below I will describe in detail how the methods work and how they have been implemented.

4.3.1 The Bootstrap Monte Carlo Method

The Bootstrap Monte-Carlo Method (Press et al., 1992) works by creating a large number of representations of the data by randomly choosing, with replacement, subsets from the original data set. This means that each newly created data set contains the same number of points as the original data set but with some points left out and some points duplicated. Now, for each dataset, the best fitting parameters are found the same way it is done with the original data and the errors are calculated from the distribution of the results. I did this in a fairly straight forward way by considering each parameter independently and thus defining the error of each parameter by taking the standard deviation of the results for this parameter produced from the artificial datasets. This procedure is valid as long as the parameters are unrelated to each other, as it is the case for the central transit time, t_c and the planetary radius r_p/r_* but one must be careful when applying this technique to

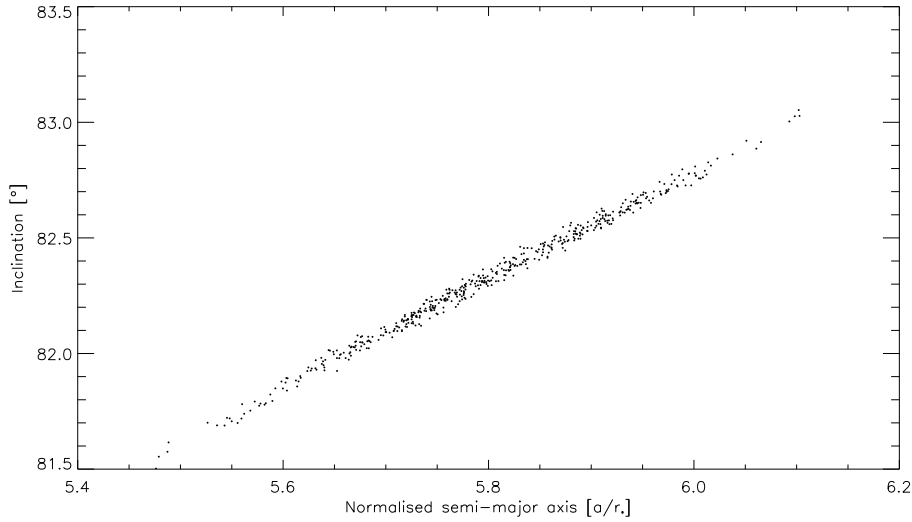


Figure 4.4: Here, the results of the Bootstrap Monte-Carlo simulation of the phased light curve in the r' -filter for the parameters a_p/r_* and inc is depicted. The degeneracy between these two parameters, namely a large separation favoring a high inclination, is clearly visible.

parameters which are degenerate meaning that e.g. a larger solution for parameter x favors a smaller solution for parameter y . In the study of transits, this is in fact the case with the semi-major axis and the inclination, since a central transit paired with a large separation produces as signal similar to that of a closer planet transiting at a lower inclination. This degeneracy can be combated by using very accurate data and exact limb darkening coefficients which allow to determine the ratio of ingress (or egress) versus the total transit time with greater accuracy. A good representation of this degeneracy can be seen in Figure 4.4 where the results of the bootstrap in the r' -filter are shown.

For the calculation of the artificial datasets, I slightly modified the routines described in section 4.2.2 in order to be accessed by a routine called *bootstrap* which was responsible for creating subsets of the data, passing them on to the subprograms and producing an output file containing the set of results from which the limits are calculated.

4.3.2 The χ^2 Surface

Based on equation 4.4, one can calculate the value of the χ^2 for any parameter input in the model. Let us assume that the model has N free parameters. Thus, we can define a function

$$f : \mathbb{R}^N \longrightarrow \mathbb{R}, \quad f(x_1, \dots, x_N) = \chi^2(x_1, \dots, x_N)$$

Transit Date	Error (bootstrap) [d]	Error ($\Delta\chi^2$) [d]
2008 01 27	0.00056	0.00052
2009 04 10	0.00055	0.00049
2009 04 15	0.00039	0.00048
2009 04 20	0.00035	0.00049
2009 04 25	0.00029	0.00035
2009 05 15	0.00031	0.00039

Table 4.1: Comparison of the errors calculated with the bootstrap and the $\Delta\chi^2$ methods. It can be seen that while they agree very well in their magnitude, the bootstrap method tends to give larger errors for the less well-sampled transits and smaller errors for the well-sampled transits compared to the errors calculated with the $\Delta\chi^2$ -method.

where $x_i, i = 1, \dots, N$ are the input parameters of the model. Since the best fit to the dataset was found by minimizing equation 4.4, the function f assumes a minimum at $\chi_{min}^2 = f(x_{1_{bf}}, \dots, x_{N_{bf}})$, where $(x_{1_{bf}}, \dots, x_{N_{bf}})$ are the best-fit parameters. Now, it is possible to find $N - 1$ -dimensional hyper-surfaces by setting

$$f(x_1, \dots, x_N) = \chi_{min}^2 + \Delta\chi^2. \quad (4.7)$$

the larger $\Delta\chi^2$ is chosen, the larger the range of (x_1, \dots, x_N) fulfilling

$$f(x_1, \dots, x_N) \leq \chi_{min}^2 + \Delta\chi^2 \quad (4.8)$$

is. Setting $\Delta\chi^2$ to a reasonable quantity and investigating the range of possible model parameters fulfilling the above criteria can be used as another way to measure the parameter errors.

To get a second estimate for the errors in the central transit time, I assumed the one-dimensional case keeping the model parameters fixed at their best values and letting t_c vary until the deviation was equal to $\Delta\chi^2 = 1$. The resulting errors are given in table 4.1. Comparing them to the errors derived with the bootstrap method, it can be seen that the errors are smaller for light curves with a lower cadence but exceed the errors calculated with the bootstrap method for the well-sampled light curves. This difference is in my opinion not to be attributed to the χ^2 -method but to the bootstrap method which overestimates the errors for not so well sampled transits. The reason for this is that the bootstrap method assumes that all points have the same impact on the fit, which is not the case for planetary transits, where e.g. a point before ingress or after egress has only limited impact on the result of the fit but points during ingress or egress carry more weight. Replacing a certain percentage of points leaves a smaller number of in-transit points for the fit as is the case for the well sampled light curves leading to an increased scatter in the outcome of the bootstrap.

Chapter 5

Results

Once the data has been recorded, reduced, analyzed and modeled, it is up to the scientist to interpret it in an astronomical fashion. In the case of this work, this encompasses putting the derived parameters into context, searching the them for any dependencies (sections 5.1.1 and 5.1.2) and comparing them with the findings of previous observations (section 5.1.3). The measurement of five new transits also allows the search for transit timing variations which might hint at additional bodies in the planetary system (section 5.2).

5.1 Planetary Parameters

Since they require high-quality observations of several transits, searches for transit timing variations enable us to refine and, if necessary re-define the parameters of the target system. For OGLE2-TR-L9, this fact is especially interesting since it is a largely unstudied system, of which so far only one full transit has been observed. To be able to compare the new parameters to the previously published values, they need to be expressed in commonly used units, removing the scaling on the stellar radius r_* . In the case of observations with GROND, we not only have one but four light curves per transit recorded in different filters allowing us to search for wavelength dependencies of the planetary parameters, especially the planetary radius which can indicate different atmospheric compositions of the planet (e.g. Lecavelier Des Etangs et al., 2008).

5.1.1 Wavelength Dependency of the Results

The first step in the analysis of the results is to compare the parameters derived from the light curves in different filters and judge if any trends are detectable. For this purpose, the results for the phased g' , r' , i' and z' light curves are presented in table 5.1 and depicted in Figures 5.1 and 5.2. While values for the normalized planetary semi-major axis and inclination found with the g' , r' and i' photometry agree within one sigma, the values derived from the z' band observations favor a larger

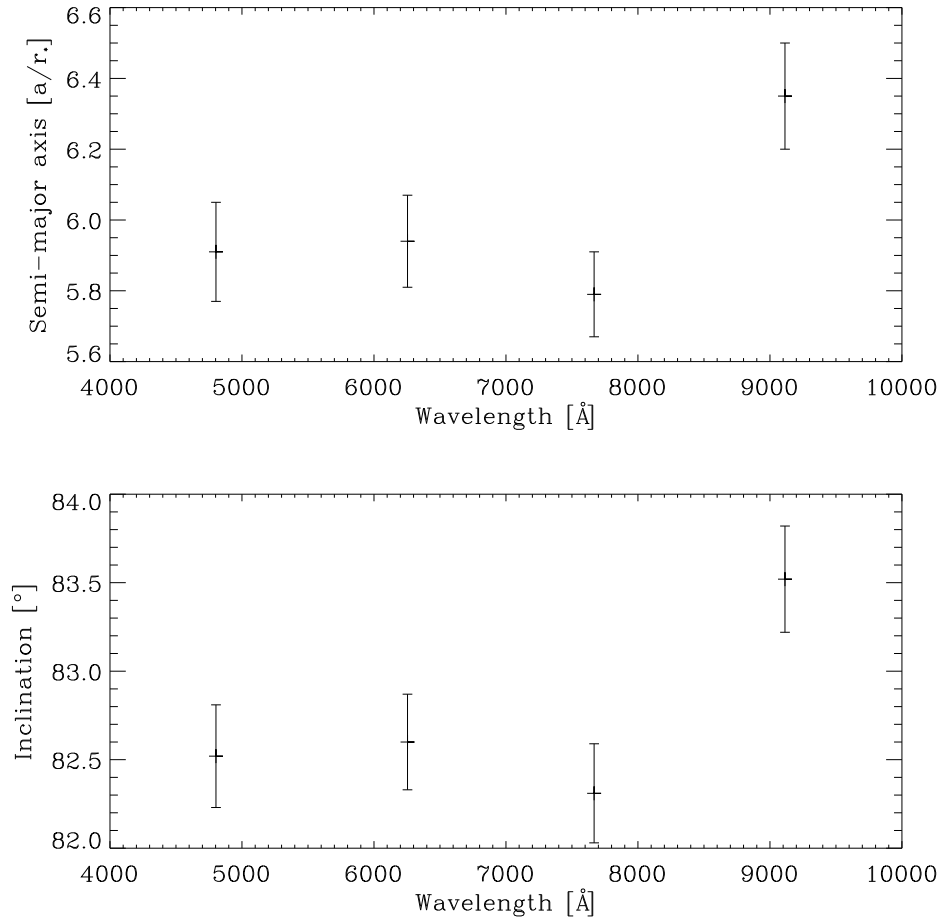


Figure 5.1: In the above Figures, the results for the planetary semi-major axis (upper panel) and the inclination (lower panel) are plotted against the central wavelength of the filters. The fact that the shapes of the variations are very similar is a clear indication for the degeneracy present between the semi-major axis and the inclination: larger solutions for the planetary separation favor higher inclinations.

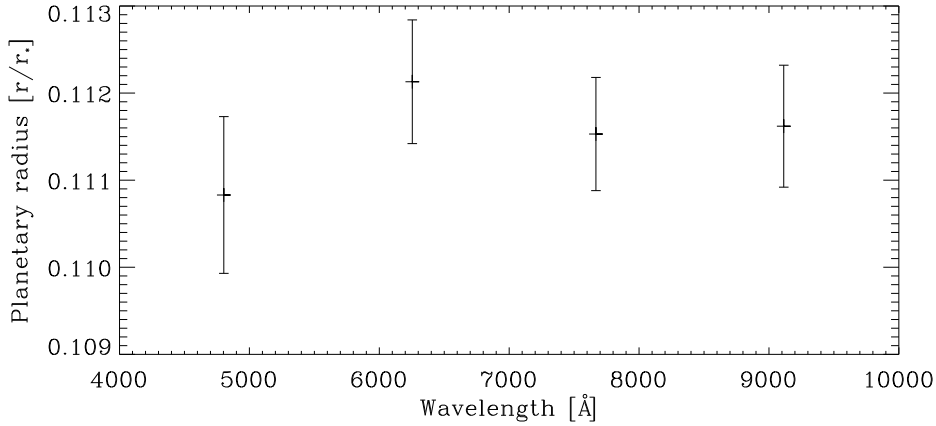


Figure 5.2: Here, the results for the radius ratio r_p/r_* is plotted against the central wavelength of the filter. All values agree within their error bars.

orbital separation combined with a higher inclination. Since there is no physical explanation for this, this tendency must be rooted either in the inferior data quality of the z' -band or in the model used to fit this light curve or a combination of the two. Since the light curve indeed has a very large scatter and limb darkening becomes small at larger wavelengths, the quadratic approximation of limb darkening might not be the ideal model for the data. To compare, I have performed a fit to the phased light curve using no limb darkening resulting in slightly different planetary parameters, $a_p/r_* = 5.99$, $r_p/r_* = 0.111922$ and $inc = 82.56^\circ$ which are compatible with the parameters found in the other band passes. With a reduced χ^2 of $\chi_{red}^2 = 1.405$ this model fits slightly better than the model including limb darkening ($\chi_{red}^2 = 1.421$). This seems to indicate that the limb darkening model for the z' -filter might not be optimal.

The most interesting parameter to investigate for variations with wavelength is the transit depth, ergo the planetary radius. Variations in the effective planetary radius reflect the transparency of the planet's atmosphere at the respective wavelengths which is influenced by the atmospheric temperature and composition. It comes in handy that the transit depth is, next to the period, the parameter which is determined with greatest accuracy. In Figure 5.2, the r_p/r_* -values are plotted against the central wavelength of the filter. This plot shows that no such variation was detected in these observations as all the values agree within their error bars.

5.1.2 Dependence on the Limb Darkening Coefficients

Although the limb darkening coefficients are not considered variables in the model, it is important to investigate if any small changes in the treatment of the limb darkening affect the outcome of the fit. For this purpose, I created a set of limb

Filter	r_p/r_*	a/r_*	inc
g'	0.11083 ± 0.00090	5.91 ± 0.14	82.52 ± 0.29
r'	0.11213 ± 0.00071	5.94 ± 0.13	82.60 ± 0.27
i'	0.11153 ± 0.00065	5.79 ± 0.12	82.31 ± 0.28
z'	0.11162 ± 0.00070	6.35 ± 0.15	83.52 ± 0.30

Table 5.1: The results computed by fitting the phased light curves for the four optical channels. The errors given are those calculated with the bootstrap Monte-Carlo method.

Parameter	Snellen et al. (2009)	This work
Semi-major axis [AU]	0.0308 ± 0.0005	0.0433 ± 0.0020
Planetary radius [R_{jup}]	1.61 ± 0.04	1.75 ± 0.05
Inclination [$^\circ$]	79.8 ± 0.3	82.3 ± 0.4
Period [d]	$2.4855335 \pm 7 \times 10^{-7}$	$2.4855349 \pm 7 \times 10^{-7}$

Table 5.2: The final results for the planetary parameters derived from the data presented in this work compared to the parameters given in Snellen et al. (2009). The values do not agree, a discussion of this divergence is presented in the text.

darkening parameters from the tables of Claret (2004) encompassing temperatures in the range of $T \in [6500, 7500]$ K, surface gravities of $\log(g) \in [4.0, 5.0]$ and metallicities of $[Fe/H] \in [-0.5, 0.5]$. These limits correspond to $[-7.6\sigma, 9.8\sigma]$, $[-4.1\sigma, 3.6\sigma]$ and $[-2.25\sigma, 2.75\sigma]$ according to the values published in Snellen et al. (2009). Then, the phased light curve in the r' -filter was fit with each of these parameters. The resulting values for a_p/r_* , r_p/r_* and inc are encompassed by 0.36σ , 0.31σ and 0.44σ of the original solutions, respectively. Still, there is a tendency towards lower reduced χ^2 - values for higher temperatures which might indicate that the stellar temperature is higher than previously determined.

5.1.3 Comparison to Previously Published Values

To find the planetary parameters a_p and r_p independent of the stellar radius r_* , I adopted the stellar parameters from Snellen et al. (2009) and combined them with the best-fit values obtained from the phased light curves. The results and their respective errors can be found in table 5.2 next to the values published by Snellen et al. (2009). It is obvious that these values do not agree, as they differ by 5.0, 3.6, 1.5 and 1.0σ for a_p , inc , r_p and t_c , respectively. I am however confident that the new values are more accurate based on the fact that we now have more data available and on the arguments presented below:

a_p Assuming the values for the period P and the stellar mass M_* from Snellen

et al. (2009), we can use Kepler's third law to calculate the planetary semi-major axis

$$P^2 = \frac{2\pi^2}{G(M_* + M_p)} a^3 \iff a = \left(\frac{P^2 G(M_* + M_p)}{4\pi^2} \right)^{1/3} \quad (5.1)$$

returning a value of 0.0413 ± 0.0008 AU. This does not agree with the value of $a_p = 0.0308 \pm 0.0005$ AU given in Snellen et al. (2009) but agrees with the value derived in this work. Since planetary motion obeys Kepler's third law, I conclude that the new value is correct.

inc Due to the degeneracy between the semi-major axis and the inclination described in section 4.3.1 a smaller semi-major axis produces a lower value for the inclination. I believe that this is the case in the analysis by Snellen et al. (2009), and therefore the discrepancy in the results for the inclination is produced by the error in the calculation of the semi-major axis or vice versa.

r_p There is also a modest discrepancy (1.5σ) in the result obtained for the planetary radius which I attribute to the increased amount of data available now.

P The period differs by one sigma from the value derived by Snellen et al. (2009). A detailed argument about the new period is given below. Although only two data points separated by several years were available back then, the period derived by Snellen et al. (2009) is quite accurate. Naturally, with the increasing number of points, the fit for the period becomes increasingly well-founded. The fact that already from two transits, the period was determined with great accuracy is due to the large time separation of these two points.

5.2 New Ephemeris and Transit Timing Variations

The motivation for our observations was to identify variations in the planetary period. To detect such variations, the central transit times of five new transits have been determined and the central transit time of one transit observed by Snellen et al. (2009) has been redetermined. From these values it is now possible to find an improved value for the planetary period as well as to search for variations from this period. In the following discussion, only the light curves obtained in the r' filter were used since they show the best quality.

5.2.1 An Improved Ephemeris

Before searching for transit timing variations, the planetary period has to be refined on the basis of the newly available data. For this purpose, I re-analyzed the transit observed by Snellen et al. (2007) and it turns out that, possibly due to an error in the HJD calculation, the central transit time is in fact HJD 2454492.80119 instead of HJD 2454492.79765. There is also an ephemeris derived by Snellen et al. (2007)

t_c [HJD - 2400000]	Reference
50478.661 ± 0.0012	Snellen et al. (2007)
54492.80119 ± 0.00056	Snellen et al. (2009)
54932.73889 ± 0.00055	this work
54937.71089 ± 0.00039	this work
54942.68182 ± 0.00035	this work
54947.65277 ± 0.00029	this work
54967.53730 ± 0.00031	this work

Table 5.3: All mid-transit times of OGLE2-TR-L9 known up to date. The first value was derived by Snellen et al. (2007) from the OGLE-II dataset and is an ephemeris based on points from several transits, the second value is the re-analyzed value of Snellen et al. (2009). The other mid-transit times are those based on observations in April and May 2009.

from the OGLE-II dataset, which I included in my analysis. It should be noted that this "mid-transit point" is the result of an analysis combining points from several different transits and thus has only limited relevance in the search for transit timing variations. All mid-transit times known for OGLE-TR-L9 can be found in table 5.3. A linear fit of all available central transit times gives the following new ephemeris:

$$T_c(E)[HJD] = 2454492.80046 + 2.4855347(\pm 6.6 \times 10^{-7})E. \quad (5.2)$$

5.2.2 Transit Timing Variations

Finally, with the new ephemeris found, it is possible to investigate for transit timing variations. To do so, the observed minus calculated (O-C) values are computed for each of the given mid-transit points. The result is plotted in Figure 5.3 while the O-C residuals are given in table 5.4. It can be seen that the transit times are not consistent with a constant period but the transit of epoch 0 (i.e. the transit observed at 27 January 2008) occurs about 1.6 minutes later than expected.

On the other hand, if the ephemeris from the OGLE-II dataset is not included in the fit for the period, an ephemeris of

$$T_c(E)[HJD] = 2454492.80140 + 2.4855285(\pm 3.2 \times 10^{-6})E. \quad (5.3)$$

is found. Based on this ephemeris, all values except the point derived from OGLE-II can be explained by a constant period. This first point shows a large deviation of 17.1 minutes which is not surprising since it was not included in the calculation of the ephemeris and is located quite far in the past. The O-C residuals for this ephemeris are given in table 5.4 while the O-C diagram is presented in Figure 5.4.

This leads to the conclusion that, if the value from OGLE-II is indeed reliable, there are indications for a variability in the period of OGLE2-TR-L9 b. However,

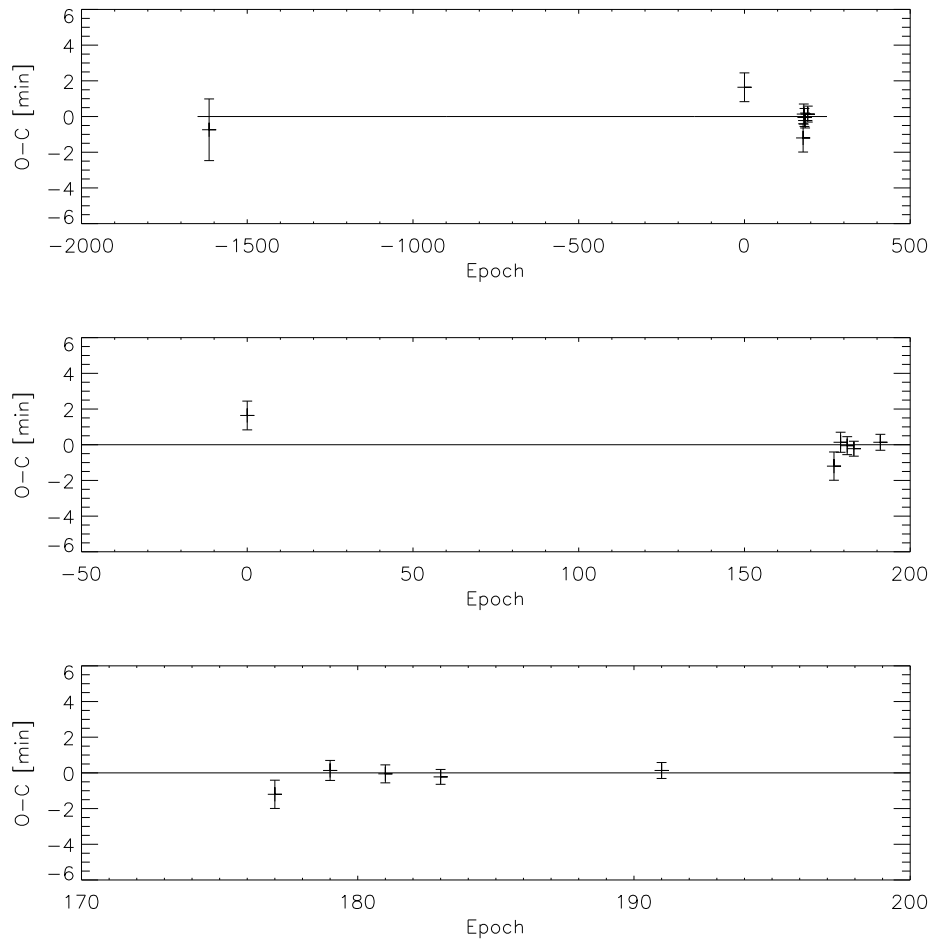


Figure 5.3: Here, the O-C diagram for the ephemeris calculated from all known mid-transit times of OGLE2-TR-L9 is presented. In the upper panel, all points are shown, while the lower two panels zoom in on the new points together with the point found from the transit in 2008 (middle panel) and solely the new points (lower panel). The mid-transit point of epoch 0 occurs 1.6 minutes later than calculated and might be hinting at variation in the planetary period.

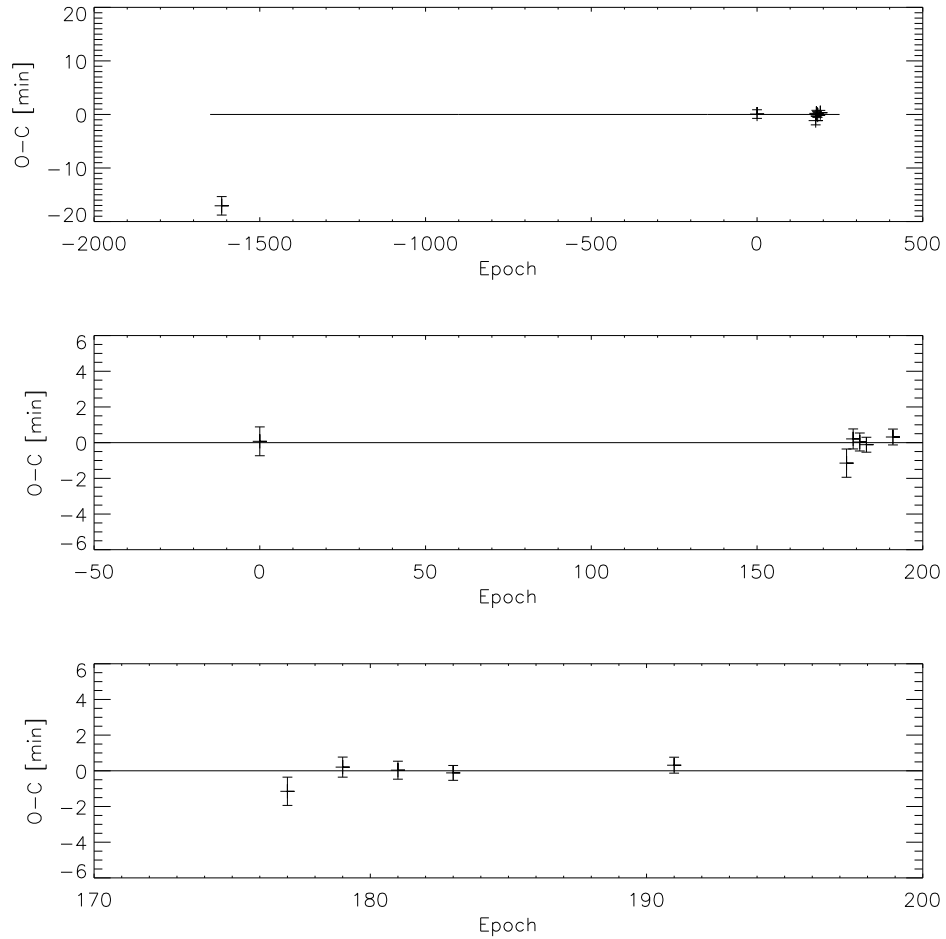


Figure 5.4: Here, the O-C diagram for the ephemeris calculated from all known mid-transit times of OGLE2-TR-L9, except the point derived from the OGLE-II data, is presented. In the upper panel, all points are shown, while the lower two panels zoom in on the new points together with the point found from the transit in 2008 (middle panel) and solely the new points (lower panel). This period explains the new points together with the point from 2008 (Epoch 0) but extrapolated to Epoch -1615 , it does not match the mid-transit time derived from the OGLE-II data.

Epoch	O-C [min] (all points)	O-C [min] (no OGLE-II)
-1615	-0.74	-17.06
0	1.64	0.07
177	-1.20	-1.15
179	0.14	0.21
181	-0.05	0.04
183	-0.22	-0.12
191	0.14	0.32

Table 5.4: This table lists the deviation of the measured mid-transit points from the periods calculated on the basis of all observed mid-transit points (central column) and all mid-transit points except for the point derived from the OGLE-II data (right column). It is logical, that the period calculated only from the new points fits them better but produces quite a large deviation for the earliest point.

since the result is based on one data point, this is no reliable detection. For the new ephemeris for the OGLE2-TR-L9 system, all data points should be taken into account (as done in 5.2.1), especially since the first point is located several years in the past, a fit including this point has a considerably higher accuracy in the prediction of future transits.

Chapter 6

Conclusion

In this work, I presented the observation of five full transits of OGLE2-TR-L9 recorded in four optical passbands with the GROND multi-channel imager. Included in the subsequent analysis is the transit obtained by Snellen et al. (2009) with the same instrument. With these new data, I recalculated the planetary parameters and searched for transit timing variations indicating the presence of additional bodies in the OGLE2-TR-L9 system. The obtained results show significant deviation from the previously published values which were based solely on the investigation of one transit. With the re-investigation of this first transit, I can be sure that this difference is not due to an actual change in the parameters of the planetary system, but to errors in the initial calculations.

The conclusion from the investigation of the calculated mid-transit times is twofold. On one hand, if one includes an ephemeris calculated from the very low-cadence OGLE-II survey, the transit times are not consistent with a constant period. On the other hand, if said point is excluded from the analysis, the O-C scatter becomes very small, showing no evidence of transit timing variations on a short timescale, but at the same time not ruling out any such variations. Thus, additional observations of the OGLE2-TR-L9 system are necessary to make a conclusive statement on the presence or absence of transit timing variations.

The transit timing technique itself holds great promises for the discovery of Earth-like planets. However, to put it into practice, one has to deal with a number of limiting factors which have so far impeded its successful application. First, the physical prerequisites for the applicability of the technique should be mentioned. While massive companions, which cause large transit timing variations in non-resonant locations, can be found more easily with the radial-velocity method, the strength of the transit timing technique lies at finding small planets located in mean motion resonances with the transiting planet. Although this seems to be a likely scenario, we can not assume that it is in fact the case for the observed systems. Another downside to the transit timing method is that, even if measurements show a varying mid-transit time, a large number of transits need to be observed in order to identify these variations as the signal of a perturbing planet. One has to face the

fact that the transit timing technique requires a large amount of observations with instruments allowing to measure the mid-transit time with good accuracy in order to be able to find small planets. This means that a large amount of observing time is required for a single discovery. However, the promise of discovering an Earth-like planet, possibly located in a habitable zone, can justify the large investment of telescope time. In my opinion, it is still not proven that the transit timing method is in fact capable of detecting planets, but I am optimistic that with the study of the Hat-P-13 system, we will be able to prove that variations in the central transit time caused by an additional planet are observable.

Bibliography

HAT website. URL <http://www.hatnet.hu/>.

KEPLER website. URL <http://kepler.nasa.gov/>.

WHAT website. URL <http://wise-obs.tau.ac.il/~what/>.

The Extrasolar Planets Encyclopaedia. URL <http://www.exoplanet.eu>.

E. Agol, J. Steffen, R. Sari, and W. Clarkson. On detecting terrestrial planets with timing of giant planet transits. *MNRAS*, 359:567–579, May 2005. doi: 10.1111/j.1365-2966.2005.08922.x.

R. Alonso, T. M. Brown, G. Torres, D. W. Latham, A. Sozzetti, G. Mandushev, J. A. Belmonte, D. Charbonneau, H. J. Deeg, E. W. Dunham, F. T. O’Donovan, and R. P. Stefanik. TrES-1: The Transiting Planet of a Bright K0 V Star. *ApJ*, 613:L153–L156, October 2004. doi: 10.1086/425256.

R. Alonso, M. Barbieri, M. Rabus, H. J. Deeg, J. A. Belmonte, and J. M. Almenara. Limits to the planet candidate GJ 436c. *A&A*, 487:L5–L8, August 2008. doi: 10.1051/0004-6361:200810007.

R. Alonso, S. Aigrain, F. Pont, T. Mazeh, and The CoRoT Exoplanet Science Team. Searching for the secondary eclipse of CoRoT-Exo-2b and its transit timing variations. In *IAU Symposium*, volume 253 of *IAU Symposium*, pages 91–96, February 2009. doi: 10.1017/S1743921308026276.

G. Bakos, C. Afonso, T. Henning, A. Jordán, M. Holman, R. W. Noyes, P. D. Sackett, D. Sasselov, G. Kovács, Z. Csubry, and A. Pál. HAT-South: A Global Network of Southern Hemisphere Automated Telescopes to Detect Transiting Exoplanets. In *IAU Symposium*, volume 253 of *IAU Symposium*, pages 354–357, February 2009a. doi: 10.1017/S174392130802663X.

G. Á. Bakos, R. W. Noyes, G. Kovács, D. W. Latham, D. D. Sasselov, G. Torres, D. A. Fischer, R. P. Stefanik, B. Sato, J. A. Johnson, A. Pál, G. W. Marcy, R. P. Butler, G. A. Esquerdo, K. Z. Stanek, J. Lázár, I. Papp, P. Sári, and B. Sipőcz. HAT-P-1b: A Large-Radius, Low-Density Exoplanet Transiting One Member of a Stellar Binary. *ApJ*, 656:552–559, February 2007. doi: 10.1086/509874.

- G. A. Bakos, A. W. Howard, R. W. Noyes, J. Hartman, G. Torres, G. Kovacs, D. A. Fischer, D. W. Latham, J. A. Johnson, G. W. Marcy, D. D. Sasselov, R. P. Stefanik, B. Sipocz, G. Kovacs, G. A. Esquerdo, A. Pal, J. Lazar, and I. Papp. HAT-P-13b,c: a transiting hot Jupiter with a massive outer companion on an eccentric orbit. *ArXiv e-prints*, July 2009b.
- G. Á. Bakos, G. Torres, A. Pál, J. Hartman, G. Kovács, R. W. Noyes, D. W. Latham, D. D. Sasselov, B. Sipőcz, G. A. Esquerdo, D. A. Fischer, J. A. Johnson, G. W. Marcy, R. P. Butler, H. Isaacson, A. Howard, S. Vogt, G. Kovács, J. Fernandez, A. Moór, R. P. Stefanik, J. Lázár, I. Papp, and P. Sári. HAT-P-11b: A Super-Neptune Planet Transiting a Bright K Star in the Kepler Field. *ArXiv e-prints*, January 2009c.
- S. Ballard, J. L. Christiansen, D. Charbonneau, D. Deming, M. J. Holman, D. Fabrycky, M. F. A’Hearn, D. D. Wellnitz, R. K. Barry, M. J. Kuchner, T. A. Livenood, T. Hewagama, J. M. Sunshine, D. L. Hampton, C. M. Lisse, S. Seager, and J. F. Veverka. A Search for Additional Planets in the NASA EPOXI Observations of the Exoplanet System GJ 436. *ArXiv e-prints*, September 2009.
- J. L. Bean. An analysis of the transit times of CoRoT-1b. *ArXiv e-prints*, March 2009.
- J. L. Bean and A. Seifahrt. Observational consequences of the recently proposed Super-Earth orbiting GJ 436. *A&A*, 487:L25–L28, August 2008. doi: 10.1051/0004-6361:200810278.
- J. L. Bean, G. F. Benedict, D. Charbonneau, D. Homeier, D. C. Taylor, B. McArthur, A. Seifahrt, S. Dreizler, and A. Reiners. A Hubble Space Telescope transit light curve for GJ 436b. *A&A*, 486:1039–1046, August 2008. doi: 10.1051/0004-6361:200810013.
- J. P. Beaulieu, D. M. Kipping, V. Batista, G. Tinetti, I. Ribas, S. Carey, J. A. Noriega-Crespo, C. A. Griffith, G. Campanella, S. Dong, J. Tennyson, R. J. Barber, P. Deroo, S. J. Fossey, D. Liang, M. R. Swain, Y. Yung, and N. Allard. Water in HD 209458b’s atmosphere from 3.6 - 8 microns IRAC photometric observations in primary transit. *ArXiv e-prints*, September 2009.
- D. P. Bennett, I. A. Bond, A. Udalski, T. Sumi, F. Abe, A. Fukui, K. Furusawa, J. B. Hearnshaw, S. Holderness, Y. Itow, K. Kamiya, A. V. Korpela, P. M. Kilmartin, W. Lin, C. H. Ling, K. Masuda, Y. Matsubara, N. Miyake, Y. Muraki, M. Nagaya, T. Okumura, K. Ohnishi, Y. C. Perrott, N. J. Rattenbury, T. Sako, T. Saito, S. Sato, L. Skuljan, D. J. Sullivan, W. L. Sweatman, P. J. Tristram, P. C. M. Yock, M. Kubiak, M. K. Szymański, G. Pietrzyński, I. Soszyński, O. Szewczyk, Ł. Wyrzykowski, K. Ulaczyk, V. Batista, J. P. Beaulieu, S. Brilliant, A. Cassan, P. Fouqué, P. Kervella, D. Kubas, and J. B. Marquette. A Low-Mass Planet with a Possible Sub-Stellar-Mass Host in Microlensing Event MOA-2007-BLG-192. *ApJ*, 684:663–683, September 2008. doi: 10.1086/589940.

- B. A. Biller, M. Kasper, L. M. Close, W. Brandner, and S. Kellner. Discovery of a Brown Dwarf Very Close to the Sun: A Methane-rich Brown Dwarf Companion to the Low-Mass Star SCR 1845-6357. *ApJ*, 641:L141–L144, April 2006. doi: 10.1086/504256.
- L. Boissard, A. Baglin, M. Auvergne, M. Deleuil, and C. Catala. Mission Profile. In M. Fridlund, A. Baglin, J. Lochar, & L. Conroy, editor, *ESA Special Publication*, volume 1306 of *ESA Special Publication*, pages 465–9, November 2006.
- I. A. Bond, A. Udalski, M. Jaroszyński, N. J. Rattenbury, B. Paczyński, I. Soszyński, L. Wyrzykowski, M. K. Szymański, M. Kubiak, O. Szewczyk, K. Żebruń, G. Pietrzyński, F. Abe, D. P. Bennett, S. Eguchi, Y. Furuta, J. B. Hearnshaw, K. Kamiya, P. M. Kilmartin, Y. Kurata, K. Masuda, Y. Matsubara, Y. Muraki, S. Noda, K. Okajima, T. Sako, T. Sekiguchi, D. J. Sullivan, T. Sumi, P. J. Tristram, T. Yanagisawa, and P. C. M. Yock. OGLE 2003-BLG-235/MOA 2003-BLG-53: A Planetary Microlensing Event. *ApJ*, 606:L155–L158, May 2004. doi: 10.1086/420928.
- X. Bonfils, T. Forveille, X. Delfosse, S. Udry, M. Mayor, C. Perrier, F. Bouchy, F. Pepe, D. Queloz, and J.-L. Bertaux. The HARPS search for southern extra-solar planets. VI. A Neptune-mass planet around the nearby M dwarf Gl 581. *A&A*, 443:L15–L18, December 2005. doi: 10.1051/0004-6361:200500193.
- P. Bordé, D. Rouan, and A. Léger. Exoplanet detection capability of the COROT space mission. *A&A*, 405:1137–1144, July 2003. doi: 10.1051/0004-6361:20030675.
- W. J. Borucki, D. Koch, J. Jenkins, D. Sasselov, R. Gilliland, N. Batalha, D. W. Latham, D. Caldwell, G. Basri, T. Brown, J. Christensen-Dalsgaard, W. D. Cochran, E. DeVore, E. Dunham, A. K. Dupree, T. Gautier, J. Geary, A. Gould, S. Howell, H. Kjeldsen, J. Lissauer, G. Marcy, S. Meibom, D. Morrison, and J. Tarter. Kepler's Optical Phase Curve of the Exoplanet HAT-P-7b. *Science*, 325:709–, August 2009. doi: 10.1126/science.1178312.
- A. Burrows, T. Guillot, W. B. Hubbard, M. S. Marley, D. Saumon, J. I. Lunine, and D. Sudarsky. On the Radii of Close-in Giant Planets. *ApJ*, 534:L97–L100, May 2000. doi: 10.1086/312638.
- R. P. Butler, G. W. Marcy, E. Williams, H. Hauser, and P. Shirts. Three New "51 Pegasi-Type" Planets. *ApJ*, 474:L115+, January 1997. doi: 10.1086/310444.
- R. P. Butler, S. S. Vogt, G. W. Marcy, D. A. Fischer, J. T. Wright, G. W. Henry, G. Laughlin, and J. J. Lissauer. A Neptune-Mass Planet Orbiting the Nearby M Dwarf GJ 436. *ApJ*, 617:580–588, December 2004. doi: 10.1086/425173.

- C. Caceres, V. D. Ivanov, D. Minniti, D. Naef, C. Melo, E. Mason, F. Selman, and G. Pietrzynski. High Cadence Near Infrared Timing Observations of Extrasolar Planets: I. GJ 436b and XO-1b. *ArXiv e-prints*, May 2009.
- J. A. Carter, J. N. Winn, R. Gilliland, and M. J. Holman. Near-Infrared Transit Photometry of the Exoplanet HD 149026b. *ApJ*, 696:241–253, May 2009. doi: 10.1088/0004-637X/696/1/241.
- D. Charbonneau, T. M. Brown, D. W. Latham, and M. Mayor. Detection of Planetary Transits Across a Sun-like Star. *ApJ*, 529:L45–L48, January 2000. doi: 10.1086/312457.
- D. Charbonneau, T. M. Brown, R. W. Noyes, and R. L. Gilliland. Detection of an Extrasolar Planet Atmosphere. *ApJ*, 568:377–384, March 2002. doi: 10.1086/338770.
- G. Chauvin, A.-M. Lagrange, C. Dumas, B. Zuckerman, D. Mouillet, I. Song, J.-L. Beuzit, and P. Lowrance. A giant planet candidate near a young brown dwarf. Direct VLT/NACO observations using IR wavefront sensing. *A&A*, 425:L29–L32, October 2004. doi: 10.1051/0004-6361:200400056.
- G. Chauvin, A.-M. Lagrange, B. Zuckerman, C. Dumas, D. Mouillet, I. Song, J.-L. Beuzit, P. Lowrance, and M. S. Bessell. A companion to AB Pic at the planet/brown dwarf boundary. *A&A*, 438:L29–L32, August 2005. doi: 10.1051/0004-6361:200500111.
- A. Claret. Non-linear limb-darkening law for LTE models. III. (Claret, 2004). *VizieR Online Data Catalog*, 342:81001–+, October 2004.
- W. D. Cochran, A. P. Hatzes, R. P. Butler, and G. W. Marcy. The Discovery of a Planetary Companion to 16 Cygni B. *ApJ*, 483:457–+, July 1997. doi: 10.1086/304245.
- J. L. Coughlin, G. S. Stringfellow, A. C. Becker, M. López-Morales, F. Mezzalana, and T. Krajci. New Observations and a Possible Detection of Parameter Variations in the Transits of Gliese 436b. *ApJ*, 689:L149–L152, December 2008. doi: 10.1086/595822.
- T. Currie and B. Hansen. The Evolution of Protoplanetary Disks around Millisecond Pulsars: The PSR 1257+12 System. *ApJ*, 666:1232–1244, September 2007. doi: 10.1086/520327.
- R. F. Díaz, P. Rojo, M. Melita, S. Hoyer, D. Minniti, P. J. D. Mauas, and M. T. Ruíz. Detection of Period Variations in Extrasolar Transiting Planet OGLE-TR-111b. *ApJ*, 682:L49–L52, July 2008. doi: 10.1086/590907.
- P. Figueira, F. Pont, C. Mordasini, Y. Alibert, C. Georgy, and W. Benz. Bulk composition of the transiting hot Neptune around GJ 436. *A&A*, 493:671–676, January 2009. doi: 10.1051/0004-6361:20078951.

- E. B. Ford and M. J. Holman. Using Transit Timing Observations to Search for Trojans of Transiting Extrasolar Planets. *ApJ*, 664:L51–L54, July 2007. doi: 10.1086/520579.
- M. Gillon, F. Pont, B.-O. Demory, F. Mallmann, M. Mayor, T. Mazeh, D. Queloz, A. Shporer, S. Udry, and C. Vuissoz. Detection of transits of the nearby hot Neptune GJ 436 b. *A&A*, 472:L13–L16, September 2007. doi: 10.1051/0004-6361:20077799.
- J. Greiner, W. Bornemann, C. Clemens, M. Deuter, G. Hasinger, M. Honsberg, H. Huber, S. Huber, M. Krauss, T. Krühler, A. Küpcü Yoldaş, H. Mayer-Hasselwander, B. Micán, N. Primak, F. Schrey, I. Steiner, G. Szokoly, C. C. Thöne, A. Yoldaş, S. Klose, U. Laux, and J. Winkler. GROND: a 7-Channel Imager. *PASP*, 120:405–424, April 2008. doi: 10.1086/587032.
- T. Guillot, A. Burrows, W. B. Hubbard, J. I. Lunine, and D. Saumon. Giant Planets at Small Orbital Distances. *ApJ*, 459:L35+, March 1996. doi: 10.1086/309935.
- B. M. S. Hansen, H.-Y. Shih, and T. Currie. The Pulsar Planets: A Test Case of Terrestrial Planet Assembly. *ApJ*, 691:382–393, January 2009. doi: 10.1088/0004-637X/691/1/382.
- G. W. Henry, G. W. Marcy, R. P. Butler, and S. S. Vogt. A Transiting “51 Peg-like” Planet. *ApJ*, 529:L41–L44, January 2000. doi: 10.1086/312458.
- M. J. Holman and N. W. Murray. The Use of Transit Timing to Detect Terrestrial-Mass Extrasolar Planets. *Science*, 307:1288–1291, February 2005. doi: 10.1126/science.1107822.
- P. Kalas, J. R. Graham, E. Chiang, M. P. Fitzgerald, M. Clampin, E. S. Kite, K. Stapelfeldt, C. Marois, and J. Krist. Optical Images of an Exosolar Planet 25 Light-Years from Earth. *Science*, 322:1345–, November 2008. doi: 10.1126/science.1166609.
- D. M. Kipping. Transit timing effects due to an exomoon. *MNRAS*, 392:181–189, January 2009. doi: 10.1111/j.1365-2966.2008.13999.x.
- H. A. Knutson, D. Charbonneau, R. W. Noyes, T. M. Brown, and R. L. Gilliland. Using Stellar Limb-Darkening to Refine the Properties of HD 209458b. *ApJ*, 655:564–575, January 2007. doi: 10.1086/510111.
- D. G. Koch, W. Borucki, L. Webster, E. Dunham, J. Jenkins, J. Marriott, and H. J. Reitsema. Kepler: a space mission to detect earth-class exoplanets. In P. Y. Bely & J. B. Breckinridge, editor, *Society of Photo-Optical Instrumentation Engineers (SPIE) Conference Series*, volume 3356 of *Society of Photo-Optical Instrumentation Engineers (SPIE) Conference Series*, pages 599–607, August 1998.

- M. Konacki, G. Torres, S. Jha, and D. D. Sasselov. An extrasolar planet that transits the disk of its parent star. *Nature*, 421:507–509, January 2003.
- A.-M. Lagrange, D. Gratadour, G. Chauvin, T. Fusco, D. Ehrenreich, D. Mouillet, G. Rousset, D. Rouan, F. Allard, É. Gendron, J. Charton, L. Mugnier, P. Rabou, J. Montri, and F. Lacombe. A probable giant planet imaged in the β Pictoris disk. VLT/NaCo deep L'-band imaging. *A&A*, 493:L21–L25, January 2009. doi: 10.1051/0004-6361:200811325.
- A. Lecavelier Des Etangs, A. Vidal-Madjar, J.-M. Désert, and D. Sing. Rayleigh scattering by H_2 in the extrasolar planet HD 209458b. *A&A*, 485:865–869, July 2008. doi: 10.1051/0004-6361:200809704.
- J. Leconte, I. Baraffe, G. Chabrier, T. Barman, and B. Levrard. Structure and evolution of the first CoRoT exoplanets: Probing the Brown Dwarf/Planet overlapping mass regime. *ArXiv e-prints*, July 2009.
- A. Leger, D. Rouan, J. Schneider, P. Barge, M. Fridlund, B. Samuel, M. Ollivier, E. Guenther, M. Deleuil, H. J. Deeg, M. Auvergne, R. Alonso, S. Aigrain, A. Alapini, J. M. Almenara, A. Baglin, M. Barbieri, H. Bruntt, P. Borde, F. Bouchy, J. Cabrera, C. Catala, L. Carone, S. Carpano, S. Csizmadia, R. Dvorkak, A. Erikson, S. Ferraz-Mello, B. Foing, F. Fressin, D. Gandolfi, M. Gillon, P. Gondoin, O. Grasset, T. Guillot, A. Hatzes, G. Hebrard, L. Jorda, H. Lammer, A. Llebaria, B. Loeillet, M. Mayor, T. Mazeh, C. Moutou, M. Paetzold, F. Pont, D. Queloz, H. Rauer, S. Renner, R. Samadi, A. Shporer, C. Sotin, B. Tingley, and G. Wuchterl. Transiting exoplanets from the CoRoT space mission VIII. CoRoT-7b: the first Super-Earth with measured radius. *ArXiv e-prints*, August 2009.
- J. J. Lissauer. Three planets for Upsilon Andromedae. *Nature*, 398:659–+, April 1999. doi: 10.1038/19409.
- K. Mandel and E. Agol. Analytic Light Curves for Planetary Transit Searches. *ApJ*, 580:L171–L175, December 2002. doi: 10.1086/345520.
- C. Marois, B. Macintosh, T. Barman, B. Zuckerman, I. Song, J. Patience, D. Lafrenière, and R. Doyon. Direct Imaging of Multiple Planets Orbiting the Star HR 8799. *Science*, 322:1348–, November 2008. doi: 10.1126/science.1166585.
- M. Mayor and D. Queloz. A Jupiter-mass companion to a solar-type star. *Nature*, 378:355–359, November 1995. doi: 10.1038/378355a0.
- M. Mayor, X. Bonfils, T. Forveille, X. Delfosse, S. Udry, J. -. Bertaux, H. Beust, F. Bouchy, C. Lovis, F. Pepe, C. Perrier, D. Queloz, and N. C. Santos. The HARPS search for southern extra-solar planets XVIII. An Earth-mass planet in the GJ 581 planetary system. *ArXiv e-prints*, June 2009.

- P. R. McCullough, J. E. Stys, J. A. Valenti, S. W. Fleming, K. A. Janes, and J. N. Heasley. The XO Project: Searching for Transiting Extrasolar Planet Candidates. *PASP*, 117:783–795, August 2005. doi: 10.1086/432024.
- E. Miller-Ricci, J. F. Rowe, D. Sasselov, J. M. Matthews, D. B. Guenther, R. Kuschnig, A. F. J. Moffat, S. M. Rucinski, G. A. H. Walker, and W. W. Weiss. MOST Space-based Photometry of the Transiting Exoplanet System HD 209458: Transit Timing to Search for Additional Planets. *ApJ*, 682:586–592, July 2008. doi: 10.1086/587446.
- C. Moutou. The Exoplanet Program of the CoRoT Space Mission. In S. Udry, W. Benz, & R. von Steiger, editor, *Planetary Systems and Planets in Systems*, pages 221–+, December 2006.
- R. Neuhauser, E. W. Guenther, G. Wuchterl, M. Mugrauer, A. Bedalov, and P. H. Hauschildt. Evidence for a co-moving sub-stellar companion of GQ Lup. *A&A*, 435:L13–L16, May 2005. doi: 10.1051/0004-6361:200500104.
- R. W. Noyes, S. Jha, S. G. Korzennik, M. Krockenberger, P. Nisenson, T. M. Brown, E. J. Kennelly, and S. D. Horner. A Planet Orbiting the Star Rho Coronae Borealis. *ApJ*, 483:L111+, July 1997. doi: 10.1086/310754.
- J. C. B. Papaloizou. Disk Planet Interactions And Early Evolution in Young Planetary Systems. *Celestial Mechanics and Dynamical Astronomy*, 91:33–57, January 2005. doi: 10.1007/s10569-004-4817-3.
- F. Pepe, M. Mayor, G. Rupprecht, G. Avila, P. Ballester, J.-L. Beckers, W. Benz, J.-L. Bertaux, F. Bouchy, B. Buzzoni, C. Cavadore, S. Deiries, H. Dekker, B. Delabre, S. D’Odorico, W. Eckert, J. Fischer, M. Fleury, M. George, A. Gilliotte, D. Gojak, J.-C. Guzman, F. Koch, D. Kohler, H. Kozlowski, D. Lacroix, J. Le Merrer, J.-L. Lizon, G. Lo Curto, A. Longinotti, D. Megevand, L. Pasquini, P. Petitpas, M. Pichard, D. Queloz, J. Reyes, P. Richaud, J.-P. Sivan, D. Sosnowska, R. Soto, S. Udry, E. Ureta, A. van Kesteren, L. Weber, U. Weilenmann, A. Wicenc, G. Wieland, J. Christensen-Dalsgaard, D. Dravins, A. Hatzes, M. Kürster, F. Paresce, and A. Penny. HARPS: ESO’s coming planet searcher. Chasing exoplanets with the La Silla 3.6-m telescope. *The Messenger*, 110: 9–14, December 2002.
- E. S. Phinney and B. M. S. Hansen. The pulsar planet production process. In J. A. Phillips, S. E. Thorsett, & S. R. Kulkarni, editor, *Planets Around Pulsars*, volume 36 of *Astronomical Society of the Pacific Conference Series*, pages 371–390, January 1993.
- D. L. Pollacco, I. Skillen, A. C. Cameron, D. J. Christian, C. Hellier, J. Irwin, T. A. Lister, R. A. Street, R. G. West, D. Anderson, W. I. Clarkson, H. Deeg, B. Enoch, A. Evans, A. Fitzsimmons, C. A. Haswell, S. Hodgkin, K. Horne, S. R. Kane, F. P. Keenan, P. F. L. Maxted, A. J. Norton, J. Osborne, N. R. Parley,

- R. S. I. Ryans, B. Smalley, P. J. Wheatley, and D. M. Wilson. The WASP Project and the SuperWASP Cameras. *PASP*, 118:1407–1418, October 2006. doi: 10.1086/508556.
- W. H. Press, S. A. Teukolsky, W. T. Vetterling, and B. P. Flannery. *Numerical recipes in C. The art of scientific computing*. 1992.
- D. Queloz, A. Eggenberger, M. Mayor, C. Perrier, J. L. Beuzit, D. Naef, J. P. Sivan, and S. Udry. Detection of a spectroscopic transit by the planet orbiting the star HD209458. *A&A*, 359:L13–L17, July 2000.
- D. Queloz, F. Bouchy, C. Moutou, A. Hatzes, G. Hébrard, R. Alonso, M. Auvergne, A. Baglin, M. Barbieri, P. Barge, W. Benz, P. Bordé, H. J. Deeg, M. Deleuil, R. Dvorak, A. Erikson, S. Ferraz Mello, M. Fridlund, D. Gandolfi, M. Gillon, E. Guenther, T. Guillot, L. Jorda, M. Hartmann, H. Lammer, A. Léger, A. Llebaria, C. Lovis, P. Magain, M. Mayor, T. Mazeh, M. Ollivier, M. Pätzold, F. Pepe, H. Rauer, D. Rouan, J. Schneider, D. Segransan, S. Udry, and G. Wuchterl. The CoRoT-7 planetary system: two orbiting super-Earths. *A&A*, 506(1):303–, October 2009.
- I. Ribas, A. Font-Ribera, and J.-P. Beaulieu. A $\sim 5M_{\oplus}$ Super-Earth Orbiting GJ 436? The Power of Near-Grazing Transits. *ApJ*, 677:L59–L62, April 2008. doi: 10.1086/587961.
- L. J. Richardson, D. Deming, K. Horning, S. Seager, and J. Harrington. A spectrum of an extrasolar planet. *Nature*, 445:892–895, February 2007. doi: 10.1038/nature05636.
- J. F. Rowe, J. M. Matthews, S. Seager, E. Miller-Ricci, D. Sasselov, R. Kuschnig, D. B. Guenther, A. F. J. Moffat, S. M. Rucinski, G. A. H. Walker, and W. W. Weiss. The Very Low Albedo of an Extrasolar Planet: MOST Space-based Photometry of HD 209458. *ApJ*, 689:1345–1353, December 2008. doi: 10.1086/591835.
- K. C. Sahu, S. Casertano, H. E. Bond, J. Valenti, T. Ed Smith, D. Minniti, M. Zoccali, M. Livio, N. Panagia, N. Piskunov, T. M. Brown, T. Brown, A. Renzini, R. M. Rich, W. Clarkson, and S. Lubow. Transiting extrasolar planetary candidates in the Galactic bulge. *Nature*, 443:534–540, October 2006. doi: 10.1038/nature05158.
- B. Sato, D. A. Fischer, G. W. Henry, G. Laughlin, R. P. Butler, G. W. Marcy, S. S. Vogt, P. Bodenheimer, S. Ida, E. Toyota, A. Wolf, J. A. Valenti, L. J. Boyd, J. A. Johnson, J. T. Wright, M. Ammons, S. Robinson, J. Strader, C. McCarthy, K. L. Tah, and D. Minniti. The N2K Consortium. II. A Transiting Hot Saturn around HD 149026 with a Large Dense Core. *ApJ*, 633:465–473, November 2005. doi: 10.1086/449306.

- T. O. B. Schmidt, R. Neuhauser, A. Seifahrt, N. Vogt, A. Bedalov, C. Helling, S. Witte, and P. H. Hauschildt. Direct evidence of a sub-stellar companion around CT Chamaeleontis. *A&A*, 491:311–320, November 2008. doi: 10.1051/0004-6361:20078840.
- A. Shporer, T. Mazeh, F. Pont, J. N. Winn, M. J. Holman, D. W. Latham, and G. A. Esquerdo. Photometric Follow-Up Observations of the Transiting Neptune-Mass Planet GJ 436b. *ApJ*, 694:1559–1565, April 2009. doi: 10.1088/0004-637X/694/2/1559.
- I. A. G. Snellen, R. F. J. van der Burg, M. D. J. de Hoon, and F. N. Vuijsje. A search for transiting extrasolar planet candidates in the OGLE-II microlens database of the galactic plane. *A&A*, 476:1357–1363, December 2007. doi: 10.1051/0004-6361:20078365.
- I. A. G. Snellen, J. Koppenhoefer, R. F. J. van der Burg, S. Dreizler, J. Greiner, M. D. J. de Hoon, T. O. Husser, T. Krühler, R. P. Saglia, and F. N. Vuijsje. OGLE2-TR-L9b an exoplanet transiting a rapidly rotating F3 star. *A&A*, 497: 545–550, April 2009. doi: 10.1051/0004-6361/200810917.
- G. S. Stringfellow, J. L. Coughlin, M. López-Morales, A. C. Becker, T. Krajci, F. Mezzalana, and E. Agol. Transit Timing Observations of the Extrasolar Hot-Neptune Planet GL 436 b. In E. Stempels, editor, *American Institute of Physics Conference Series*, volume 1094 of *American Institute of Physics Conference Series*, pages 481–484, February 2009. doi: 10.1063/1.3099153.
- M. R. Swain, G. Vasisht, and G. Tinetti. The presence of methane in the atmosphere of an extrasolar planet. *Nature*, 452:329–331, March 2008. doi: 10.1038/nature06823.
- E. W. Thommes. A Safety Net for Fast Migrators: Interactions between Gap-opening and Sub-Gap-opening Bodies in a Protoplanetary Disk. *ApJ*, 626:1033–1044, June 2005. doi: 10.1086/429913.
- G. Tinetti, A. Vidal-Madjar, M.-C. Liang, J.-P. Beaulieu, Y. Yung, S. Carey, R. J. Barber, J. Tennyson, I. Ribas, N. Allard, G. E. Ballester, D. K. Sing, and F. Selsis. Water vapour in the atmosphere of a transiting extrasolar planet. *Nature*, 448:169–171, July 2007. doi: 10.1038/nature06002.
- D. Tody. IRAF in the Nineties. In R. J. Hanisch, R. J. V. Brissenden, & J. Barnes, editor, *Astronomical Data Analysis Software and Systems II*, volume 52 of *Astronomical Society of the Pacific Conference Series*, pages 173–+, January 1993.
- G. Torres, J. N. Winn, and M. J. Holman. Improved Parameters for Extrasolar Transiting Planets. *ApJ*, 677:1324–1342, April 2008. doi: 10.1086/529429.

- A. Udalski, M. Kubiak, and M. Szymanski. Optical Gravitational Lensing Experiment. OGLE-2 – the Second Phase of the OGLE Project. *Acta Astronomica*, 47: 319–344, July 1997.
- A. Udalski, K. Zebrun, M. Szymanski, M. Kubiak, I. Soszynski, O. Szewczyk, L. Wyrzykowski, and G. Pietrzynski. The Optical Gravitational Lensing Experiment. Search for Planetary and Low-Luminosity Object Transits in the Galactic Disk. Results of 2001 Campaign – Supplement. *Acta Astronomica*, 52:115–128, June 2002.
- A. Udalski, G. Pietrzynski, M. Szymanski, M. Kubiak, K. Zebrun, I. Soszynski, O. Szewczyk, and L. Wyrzykowski. The Optical Gravitational Lensing Experiment. Additional Planetary and Low-Luminosity Object Transits from the OGLE 2001 and 2002 Observational Campaigns. *Acta Astronomica*, 53:133–149, June 2003.
- S. Udry, X. Bonfils, X. Delfosse, T. Forveille, M. Mayor, C. Perrier, F. Bouchy, C. Lovis, F. Pepe, D. Queloz, and J.-L. Bertaux. The HARPS search for southern extra-solar planets. XI. Super-Earths (5 and 8 M_{\oplus}) in a 3-planet system. *A&A*, 469:L43–L47, July 2007. doi: 10.1051/0004-6361:20077612.
- W. F. Welsh. Transit Timing Variations: Hints of a Second Planet in the HD 17156 System. In *Bulletin of the American Astronomical Society*, volume 41 of *Bulletin of the American Astronomical Society*, pages 373–+, January 2009.
- A. Wolszczan and D. A. Frail. A planetary system around the millisecond pulsar PSR1257 + 12. *Nature*, 355:145–147, January 1992. doi: 10.1038/355145a0.

Acknowledgments

Zunächst möchte ich mich bei meinen Eltern bedanken. Bei meinem Vater, der mich leider nur eine kurze Zeit begleiten konnte aber schon in Kindertagen meine Neugierde an Natur und Wissenschaft geweckt hat. Ein großes Dankeschön an meine Mutter Inge, die mich stets ermutigt hat, meinen Interessen zu folgen, und die mich immer tatkräftig unterstützt hat. Auch meinen Geschwistern, Barbara, Otmar und Bernhard einen Dank für unzählige Einladungen und noch unzähligere Tassen Kaffee.

A special mention goes to Klaas Vantournhout, thank you for accompanying me throughout the last year. Thanks for taking the trip to Vienna again and again and for many late phone calls. Thank you for being there.

I would also like to thank my supervisors. Thanks to Cristina Afonso for making it possible for me to work at the Max Planck Institute for Astronomy and for her advice and guidance. And to Gerald Handler who not only always found a desk for me in Vienna but who has taught me a great deal about Astronomy and given me many pieces of good advice.

Cheers to the members of the transiting planets group in Heidelberg for welcoming me among them. Special credit goes to Nikolay Nikolov who taught me how to fit planetary transits and who was a great help during my first months in Heidelberg. Thanks to Johannes Koppenhoefer who introduced me to the GROND instrument and shared many tricks with me. A round of thanks also goes to the Gamma-Ray-Burst observers who were very helpful during the observing run and recorded a transit for me.

Monika Lendl

Curriculum Vitae

✉ lendl@mpia.de

Personal Information

Date of Birth December 31, 1984
Place of Birth Salzburg, Austria
Nationality Austrian

Education

1995–2003 **Qualification for University Entrance (Matura)**, *Bundesgymnasium Nonntal*, Salzburg, Austria.
Completed with distinction.

2004 **Arts (Various Courses)**, *University of New South Wales*, Sydney, Australia.
Member of Goldstein College.

2004–2007 **Bachelor of Science (Astronomy)**, *University of Vienna*, Vienna, Austria.
Thesis topic: “Hot Jupiters”, supervisor: R. Dvorak.

2006–present **Mathematics**, *University of Vienna*, Vienna, Austria.

2007–present **Astronomy (Master)**, *University of Vienna*, Vienna, Austria, *Max Planck Institute for Astronomy*, Heidelberg, Germany.
Study foci: Stellar Astronomy and Astrophysics, Planetology and Dynamical Astronomy.
The research work is carried out at MPIA.

Master thesis

title *Search for Additional Bodies with the Transit Timing Method*
supervisors Cristina Afonso (MPIA), Gerald Handler (Univ. of Vienna)

description Among the ever growing number of extrasolar planets, planets which pass in front of their parent stars constitute an especially interesting class. During the transit a small decrease in the stars apparent brightness can be observed allowing us to measure properties inaccessible in other ways or improve on values previously determined. One of the properties that can be measured with great accuracy is the transit midpoint and consequently the planetary period. If a planetary system contains additional massive objects such as moons or undetected planets, dynamical interactions between these bodies can cause considerable variations in the planetary period. I probe two transiting systems for such variations.

Experience

Research

- 2007–present **Observer**, *University Observatory Vienna*, Vienna, Austria.
Search for and study of pulsating stars.
- 2007–present **Observer**, *University Observatory Vienna*, Vienna, Austria.
Follow-up observations for the CoRoT satellite.
- 2009 **Observer**, *Max Planck Institute for Astronomy*, Heidelberg, Germany.
Spectroscopic and photometric observations during a 19-night run at the MPG/ESO 2.2m telescope at La Silla.

Other

- 2006–2007 **Lab Demonstrator**, *University of Vienna*, Vienna, Austria.
Supervision of a group of students during the lecture “Introduction to Astronomy”.
- 2007 **Participant**, *Summer School “Tandem”*, Nizhny Novgorod, Russia.
Language school (Russian).
- 2007, 2008 **Participant**, *International Astronomical Youth Camp*.
Projects completed in the fields of general relativity (2007) and super-dense matter (2008).
- 2009–present **Co-Organizer**, *International Astronomical Youth Camp*.
Organisation of sponsorship and advertisement.
Supervision of a working group during the camp.

Languages

German	native language	Russian	moderate
English	excellent	Dutch	basic
Spanish	fluent	French	basic

Interests

- Extrasolar Planets Extrasolar planets have always been the field which I am most keenly interested in. It is extremely dynamic with new discoveries chasing one another showing that we still are far away from a complete understanding of planetary systems. I am interested in both, the theoretical and the observational approaches to studying these strange new worlds.
- Young Stars The above topic is closely related to the process of star formation itself. Here, my interest lies mainly on the lower mass range (T Tauri stars).
- Observational Astronomy I am very curious to learn more about the technical side of Astronomy. Only with inventive instrumentation and exact observational techniques can we advance in the study of astronomical objects.

Publications

G. Handler, J. L. Provencal, M. Lendl, M. H. Montgomery, P. Beck, 2008. Constraining convection parameters from the light curve shapes of pulsating white dwarf stars: the cases of ec 14012-1446 and wd 1524-0030. *Journal of Physics: Conference Series*, **118**, 012057pp.

G. Handler, J. L. Provencal, M. H. Montgomery, E. Romero-Colmenero, K. Sanchawala, M. Lendl, M. A. Wood, I. Silver, P. Beck, and W.-P. Chen, 2008. A three-site photometric campaign on the zz ceti star wd 1524-0030. *Communications in Asteroseismology*, **56**, 18–26.

H. J. Deeg, M. Gillon, A. Shporer, D. Rouan, B. Stecklum, S. Aigrain, A. Alapini, J.M. Almenara, R. Alonso, M. Barbieri, F. Bouchy, J. Eislöffel, A. Erikson, M. Fridlund, P. Eigmüller, G. Handler, A. Hatzes, P. Kabath, M. Lendl, T. Mazeh, C. Moutou, D. Queloz, H. Rauer, M. Rabus, B. Tingley, and R. Titz, 2009. Ground-based photometry of space-based transit detections: Photometric follow-up of the CoRoT mission. *Astronomy & Astrophysics*, accepted.

M. Lendl, C. Afonso, J. Koppenhoefer, N. Nikolov, T. Henning, 2009. New Parameters of OGLE2-TR-L9 Based on Multicolor Observations. in prep.